Title
Virtual 3D Orthognathic Treatment Simulation Accuracy: Comparison of Prediction and Surgical Outcome

Author
Shanahan, Ken

Publication Date
2011

Peer reviewed|Thesis/dissertation

Virtual 3D Orthognathic Treatment Simulation Accuracy: Comparison of Prediction and Surgical Outcome

by

Kenneth Francis Shanahan, DDS

THESIS

Submitted in partial satisfaction of the requirements for the degree of

MASTER OF SCIENCE

in

Oral and Craniofacial Sciences

in the

DEDICATION

I would like to dedicate this thesis to my wife, Alyson, who has been my constant companion and support during my education. Her dedication to the raising of our children, Finnegan and Ivy, in my many absences, whether physical or mental, has made it possible for me to complete my educational pursuits. I would be less the man I am today without her encouragement and support. I love her very much and thank her for the countless ways she has sacrificed during these past years. I also wanted to dedicate this thesis to my children. They have brought joy to my life and provided me with a wonderful perspective with which to approach every day.

ACKNOWLEDGEMENTS

I would like to acknowledge a few people who made this work possible. Firstly, I'd like to acknowledge Dr. John Huang. Dr. Huang has been a great asset to the research pursuits at UCSF in the realm of cone beam CT imaging, and my thesis was no exception. Dr Huang's extensive knowledge of the 3D imaging field and his innovative ideas tremendously helped me in this endeavor. Dr Janice Lee was also an exceptional mentor, providing her extensive database of orthognathic surgical cases to use for the project, as well as serving as a knowledgebase for my many surgical questions and in analysis of the results. I have been extremely fortunate to have had the opportunity to work with these wonderful mentors.

Dr. Art Miller was a great source of guidance and encouragement. His enthusiasm for my project gave me the drive to continue to work diligently on each step of the work. His friendly reminders for due dates also helped to keep me on track.

Also, Dr. Sona Bekmezian was a tremendous asset in the painstaking process of picking landmarks for testing the orientation methods, as well as in many data mining procedures. Without her help, I would have been forced to decrease the breadth of this study. She was incredibly patient and an integral member of the team.

ABSTRACT

Virtual 3D Orthognathic Treatment Simulation Accuracy:

Comparison of Prediction and Surgical Outcome

Kenneth Francis Shanahan, DDS

Introduction: Cone beam computed tomography (CBCT) technology has many known benefits in diagnosis and treatment planning. One area in early development is the use of CBCT in virtual orthognathic surgical simulation. The purpose of this study was to evaluate the accuracy of this technique in single jaw surgery performed by a single surgeon using a commercially available software package, InVivoDental v5.1 (Anatomage, San Jose, CA USA).

Methods and Materials: Presurgical CBCT scans of 19 patients who had undergone single jaw orthognathic surgery (9 maxillary LeFort I; 10 mandibular BSSO) were segmented, retrospectively, to create 3D models. Virtual surgery was performed using the surgical notes as a guide. The post-surgery scan and the pre-surgery scan were superimposed on the anterior cranial base to measure the differences between the simulation and the actual surgical outcomes.

Results: Mean linear differences were found to be 0.51 mm horizontally, 1.07 mm anteroposteriorly, and 1.20 mm vertically. Mean rotational differences were found to be 1.41° around the z axis (yaw), 0.64° around the y axis (roll), and 1.96° around the x axis (pitch).

Conclusions: Virtual simulation of orthognathic surgery using Anatomage InVivo software closely approximates the final outcome. This protocol can be used as a tool for surgical planning and splint fabrication with the addition of improved occlusal morphology from another source.

Table of Contents

DEDICATION III

ACKNOWLEDGEMENTS IV

ABSTRACT V

LIST OF TABLES VII

LIST OF FIGURES VII

INTRODUCTION 1

Hard Tissue Predictions 1

Soft Tissue Predictions 4

Conventional Model Surgery 5

Landmark Error 6

Superimposition 8

Virtual Surgery Simulation 10

Purpose 13

Specific Aims 13

HYPOTHESIS 13

METHODS AND MATERIALS 14

Subjects 14

Landmarks 16

RESULTS 36

DISCUSSION 52

CONCLUSIONS 60

REFERENCES 61

APPENDICES 65

List of Tables

Table 1. Subjects for Retrospective Study 15
Table 2. Three-dimensional landmark definitions used for the orientation protocols. 17
Table 3. Table of results of the orientation protocols for rater 1. 37
Table 4. Table of results of the orientation protocols for rater 2. 38
Table 5. Table showing the linear difference of the mean centroids of the original scans to the superimposed scans in the x, y, and z axis over the three superimposition time points. 422
Table 6. Comparison of prediction to postsurgical outcome showing linear, vector and angular differences. 43
Table 7. Actual surgical change performed as measured from T0 to T1 (T0-T1). 44
Table 8. Linear difference of prediction to postsurgical landmarks with mean and magnitude of the mean differences (mean of the absolute value of the difference) for each axis along with the standard deviations listed. 45
Table 9. Linear differences between prediction and postsurgical outcome showing maxillary surgeries, mandibular surgeries, and the overall results for all surgeries. 488
Table 10. Angular differences between prediction and postsurgical outcom. 511
Table 11. Comparison of maxillary and mandibular surgeries. 522

List of Figures

Figure 1. Table from Kaipatur et al., 2009 showing the mean and standard deviations of the differences between prediction using a lateral headfilm and the actual postsurgical outcome. ... 2
Figure 2. Region used for superimposition in growing subjects (Cevidanes, Heymann et al.,. 2009) A, Superior view; B, inferior view. 9
Figure 3. Orientation 1: Modified Frankfort Horizontal 18
Figure 4. Orientation 2: Anatomage Default 19
Figure 5. Orientation 3: UCSF Planar View. Top) Volume rendering of a patient oriented to Orientation 3. Bottom) Planar views for completing the orientation protocol. 20
Figure 6. NFZ Based Orientation 21
Figure 7. Flowchart of the methods used to compare the virtual predictions to the postsurgical outcome 22
Figure 8. Example of a volumetric view with segmented maxilla and mandible (Anatomodels). 23

Figure 9. A) Presurgical scan with segmentation to show an example of a LeFort I maxillary advancement simulation. B) Simulation of maxillary LeFort I advancement 244
Figure 10. Frontal view of Anatomodels demonstrating the orange coloration of the maxillary dentition..... 24
Figure 11. Sagittal view of Anatomodels demonstrating that clipping parallel to the occlusal plane allows for better visualization through the teeth to evaluate for heavy posterior contacts 26
Figure 12. A) Sagittal view demonstrating the placement of the widget through the condylar hinge axis. B) Axial view demonstrating the placement of the widget through the condylar hinge axis 27
Figure 13. Result of 5 pt registration. Postsurgical volume shown in blue. Postsurgical model too far to the patient's right: requires slight manual adjustment..... 28
Figure 14. Manual adjustment of the superimposition of the postsurgical scan (shown in blue). The presurgical scan is held constant while the postsurgical scan is moved relative to the presurgical scan and its corresponding coordinate system..... 29
Figure 15. Example demonstrating the placement of the volume to be used for the superimposition, centered at anterior sella. 30
Figure 16. Completed superimposition by volume of interest. 30
Figure 17. Volumetric views of original scan (white) and superimposition scan (blue) and resulting superimposition. Landmarks were chosen on each scan separately and 3D coordinates recorded..... 31
Figure 18. Volumetric views of the dry skulls with metallic markers visible, original scan (white), blue scan (superimposition scan), and a close-up view of the center of the marker representing B point digitally identified. 32
Figure 19. Example of a maxillary surgery in which landmarks were identified on the mesial buccal cusps of the maxillary molars and at the contact point of the central incisors. 32
Figure 20. A) Model of maxilla with volumes hidden and landmarks identified. B) Prediction of maxilla position (maxillary advancement and rotation) with landmarks chosen to duplicate the position of the landmarks in T0 33
Figure 21. Plot of 3D coordinates from one surgery (Mn1). A) Z axis set to zero, and x,y coordinates plotted. Difference in yaw is 2.68° B) X axis set to zero, and y,z coordinates plotted. Difference in pitch is 1.31°. C) Y axis set to zero, and x, z coordinates plotted. Difference in roll is 0.95°. Graphics demonstrate the corresponding volumetric views for each plot. 35
Figure 22. Orientation 1 coordinate system. 36
Figure 23. The mean error for each of the four orientation methods as completed by rater 1. . 39
Figure 24. The mean error for each of the four orientation methods as completed by rater 1 .. 40
Figure 25. Overall error for each of the four orientation methods including data from both raters. 40
Figure 26. Figure demonstrating the mean error and the range of error in the x, y, and z axis between the superimposed volume to the original volume over the three time points. 41
Figure 27. Linear difference of prediction to postsurgical landmarks 45
Figure 28. Linear differences of prediction and postsurgical outcome according to axis 477

Figure 29. Absolute value of the linear differences between prediction and postsurgical outcome according to axis demonstrating relative magnitude of the differences. 488
Figure 30. Angular differences of prediction and postsurgical outcome according to axis..... 49
Figure 31. Absolute value of the angular differences between prediction and postsurgical outcome according to axis demonstrating the relative magnitude of the differences. 500

INTRODUCTION

As the popularity of cone beam computed tomography (CBCT) continues to rise, it has been shown that CBCT technology has many benefits in the areas of diagnosis and treatment planning (Mah, Huang et al. ; Hatcher and Aboudara 2004; Mah and Hatcher 2004; Miller, Maki et al. 2004). One area in early development is the use of CBCT in virtual orthognathic surgical simulation. Powerful software packages have recently become available which allow clinicians to manipulate the CBCT data in more useful ways for planning orthognathic surgery and evaluating treatment results.

Hard Tissue Predictions

Patients with severe skeletal discrepancies may require orthognathic surgery for treatment. With the advent of rigid fixation, orthognathic surgery outcomes have become more stable(Proffit, Turvey et al. 2007) and, thus, a major component of our treatment options for our patients. Conventionally, two dimensional radiographs and plaster models are used to plan the surgery. A lateral cephalogram and photos can be used with current software programs to produce a prediction of the hard and soft tissue results of surgery. The accuracy of these predictions has been extensively studied, as have the software programs used for the predictions. According to a systematic review, (Kaipatur, Al-Thomali et al. 2009), hard tissue predictions based on lateral headfilms have been shown to provide results within 2 mm and 2 degrees of accuracy, which has been deemed clinically insignificant (Donatsky, Bjorn-Jorgensen et al. 1997). The key results from the studies included in this systematic review are shown in Figure 1.

Table 4. KEY MEASUREMENT POINTS FROM SELECTED STUDIES

Study	Horizontal Measurements		Vertical Measurements	
	Mean (SD)	*P* Value	Mean (SD)	*P* Value
Skeletal measurements of anterior maxilla				
Anterior nasal spine				
Donatsky et al[78]	0.2 (1.5)	NS	0.1 (0.8)	NS
Hillerup et al[80]	<0.1 (0.7)	NS	0.5 (1.2)	NS
Donatsky et al[77]	<0.1 (1.2)	NS	−0.4 (0.5)	<.01
Donatsky et al[77]	−0.7 (0.7)	<.001	−1.0 (0.8)	<.001
Csaszar and Niederdellmann[76]	0.6 (0.6)	<.05	0.6 (0.4)	NS
Point A				
Csaszar and Niederdellmann[76]	0.6 (0.5)	NS	0.9 (0.7)	<.05
Jacobson and Sarver[59]	−0.5 (1.6)	NS	0.5 (1.4)	NS
Semaan and Goonewardene[79]	−0.3 (2.6)	NS	0.3 (2.0)	NS
Skeletal measurements of posterior maxilla				
Mx1				
Donatsky et al[78]	0.1 (1.1)	NS	<−0.1 (0.8)	NS
Donatsky et al[77]	0.0 (1.7)	NS	<0.1 (1.5)	NS
Donatsky et al[77]	−1.2 (1.5)	<.01	−0.2 (1.4)	NS
Posterior nasal spine				
Hillerup et al[80]	0.7 (1.5)	<.05	−0.6 (1.4)	NS
Csaszar and Niederdellmann[76]	0.8 (0.5)	NS	0.6 (0.5)	NS
Palatal plane				
Jacobson and Sarver[59]	−0.7 (2.8)	<.05		
Semaan and Goonewardene[79]	−1.01 (2.9)	<.05		
Skeletal measurements of anterior mandible				
Condylion-gnathion distance				
Donatsky et al[78]	−0.3 (1.3)	NS	−0.4 (0.7)	NS
Donatsky et al[77]	−0.1 (1.3)	NS	−0.0 (1.1)	NS
Donatsky et al[77]	0.9 (1.0)	<.001	−0.1 (0.8)	NS
Gnathion				
Hillerup et al[80]	−0.4 (1.3)	NS		
Csaszar and Niederdellmann[76]	1.2 (0.6)	NS	1.0 (0.9)	<.05
Pogonion				
Hillerup et al[80]	−0.4 (1.9)	NS		
Csaszar and Niederdellmann[76]	1.1 (0.5)	NS	1.3 (1.0)	NS
Menton				
Csaszar and Niederdellmann[76]	1.6 (0.8)	NS	0.9 (0.9)	<.05
Point B				
Csaszar and Niederdellmann[76]	0.9 (0.6)	NS	1.7 (1.5)	<.05
Dental measurements				
Incisor superior				
Hillerup et al[80]	−0.2 (1.3)	NS	0.4 (1.2)	NS
Donatsky et al[78]	−0.3 (1.5)	NS	−0.4 (0.7)	<.05
Donatsky et al[77]	−0.1 (0.9)	NS	−0.8 (0.9)	<.001
Csaszar and Niederdellmann[76]	0.7 (0.5)	NS	0.8 (0.6)	<.05
Jacobson and Sarver[59]	−0.4 (1.9)	NS	0.3 (1.6)	NS
Semaan and Goonewardene[79]	−0.1 (2.6)	NS	0.4 (1.9)	NS
Incisor inferior				
Hillerup et al[80]	0.1 (1.3)	NS	−0.2 (1.3)	NS
Donatsky et al[77]	−0.7 (1.3)	NS	−0.2 (1.3)	NS
Donatsky et al[77]	−0.2 (1.1)	NS	−0.4 (1.0)	NS
Csaszar and Niederdellmann[76]	0.9 (0.5)	NS	0.7 (0.4)	<.05
Molar superior				
Csaszar and Niederdellmann[76]	1.8 (1.9)	NS	1.1 (1.1)	NS
Jacobson and Sarver[59]	−0.4 (1.9)	NS	1.0 (1.3)	<.05
Semaan and Goonewardene[79]	0.0 (2.5)	NS	−0.5 (1.6)	<.05

Abbreviation: NS, not significant; Mx1, upper incisor; Mn1, lower incisor.

Figure 1. Table from Kaipatur *et al.,* 2009 showing the mean and standard deviations of the differences between prediction using a lateral headfilm and the actual postsurgical outcome.

Kaipatur et al found that the anterior maxilla has been shown to be consistent in prediction. The anterior nasal spine (ANS) was shown in most of the studies to have

insignificant differences between actual and prediction, with the exception of Csaszar and Niederdellmann and Donatsky in the horizontal direction and Donatsky in the vertical (Kaipatur and Flores-Mir 2009). Also, A point was consistently measured as an insignificant difference between actual and predicted value except Csaszar and Niederdellmann showed significance in the vertical direction. The posterior maxilla showed consistency in prediction except for Donatsky *et al.,* for the upper incisor and Hillerup *et al.,* for the posterior nasal spine (PNS). For the anterior mandible, all the studies found no significant difference in the horizontal axis of the anterior mandible position except for the condylion-gnathion distance, which was significantly different. In the vertical direction, Csaszar and Niederdellmann 00 showed statistically significant differences for all the points in the anterior mandible with differences in the prediction and actual outcomes for the gnathion, menton, and point B (Csaszar and Niederdellmann 00).

Although there was no consistency in the results for prediction of SNA and SNB, all the differences were within 1.2° of the actual mean. Of the other measurements reported, lower incisor–APog angle, lower incisor to mandibular plane, SN–mandibular plane, SN–maxillary plane, and pogonion all showed no significant differences in the reported studies. Overall, the review showed that the difference between the computer prediction and actual outcome was less than 2 mm or 2 degrees, which can be considered clinically insignificant (Kaipatur and Flores-Mir 2009).

In essence, it can be considered that software programs adequately predict the AP position of the maxilla and mandible, but vertical positions were not as accurately predicted. In many of the studies, the anterior maxilla was placed more superiorly than the predicted position, resulting in increased autorotation of the mandible which could explain the differences in the vertical position of the mandibular incisors. The final position of the maxilla appears to be

more consistently predicted for a maxillary impaction than when surgically placed caudally (downgrafted). The posterior maxilla was positioned more inferiorly than predicted by software programs (Kaipatur and Flores-Mir 2009).

In a comparison of two surgical teams with a sample size of 42 Le Fort I patients with or without a mandibular surgery, Semaan *et al.,* (Semaan and Goonewardene 2005) found that overall 66% of the postsurgical results were within 2 mm of prediction, and 26% of the results were within 1 mm of prediction using QuichCeph software. For surgery performed in a private practice, approximately three-quarters (74%) of the subjects had their maxilla placed within 2 mm of the prediction and about one-third (30%) of the maxillae were placed within 1 mm. For surgery performed in the teaching hospital, 50% of the patients had their maxilla placed within 2 mm of prediction, and 22% were placed within 1 mm. Statistically significant differences were found between the predicted and actual postsurgical maxillary molar vertical position, and significant differences were also found for the palatal plane angular measurements. When single-jaw and bimaxillary surgery were compared, no significant differences were found. Also, there were no statistically significant differences found when assessing the primary direction of movement (impaction vs downgraft vs advancement).

Jacobson, in 2002, found that in 80% of 46 patient surgical predictions, the results of the surgery were within 2 mm of the prediction (Jacobson and Sarver 2002). There were statistical differences between two surgeons in the direction of specific landmark discrepancies but not in the amount.

Soft Tissue Predictions

Soft tissue predictions based on photos and lateral cephalograms have also been shown to be valuable for treatment planning as well as presentation to patients (Mankad, Cisneros et al. 1999). To create soft tissue predictions, algorithms have been used to link the underlying

hard tissue movements to the overlying soft tissue (Smith, Thomas et al. 2004; Pektas, Kircelli et al. 2007). It has been shown that patients benefit from viewing predictions of soft tissue changes as it can help them to understand the severity of their malocclusion and the importance of a surgical treatment (Phillips, Hill et al. 1995).

There has been some debate regarding the effects of showing soft tissue predictions to patients prior to surgery. Some clinicians feel that this should be avoided so that the patient does not have unrealistic expectations for the surgery. Sarver *et al.,* found that 89% of a sample of 18 patients felt the predicted images were realistic and that the desired results were achieved. Findings support the contention that patients who have been shown treatment simulations have more realistic expectations of the treatment outcome and, therefore, the chances of dissatisfaction are reduced (Sarver, Johnston et al. 1988). In addition, Kiyak's studies show that less than 45% of patients from a nonimaged population expressed esthetic satisfaction (Kiyak and Bell 1991).

In a study designed to evaluate the subjective accuracy of soft tissue predictions, Chew *et al.,* reported that laypersons found the soft tissue prediction to be more esthetic than the actual postsurgical face in approximately 25% of the 40 cases displayed. According to these findings, there is a 25% chance that the esthetic result perceived by the patient is inferior to what could have been demonstrated during the treatment planning stage (Chew, Koh et al. 2008).

Conventional Model Surgery

The hard and soft tissue predictions allow for planning of the overall movements, but for the precise planning of the positioning of the jaws in relation to each other, mock surgery is performed on plaster models. The mock surgery also provides the splint(s) which will relate the upper and lower jaws during the surgery. This method has been considered the gold standard,

but its limitations have been identified (Ellis 1990; Choi, Song et al. 2009). For one, the dentition serves as a guide for the splint fabrication but the underlying skeletal components are not available for assessment during the model surgery (Ellis 1990; Proffit, White et al. 2002). It is a manual process that can include errors from improper mounting of the casts, inaccuracy of the intermediate wafer (Sharifi, Jones et al. 2008), the placement of reference lines on the casts, and errors in measuring the surgical displacement (Ellis 1990; Olszewski and Reychler 2004). In measuring surgical displacements in a planned model surgery, the measurements should be made from the dentition and not the reference lines; otherwise error can be introduced especially if the occlusal plane will be altered. Ellis gives the example of posterior maxillary impaction in which the anterosuperior aspect of the maxilla is moved forward. If measurements were taken at the level of the planned osteotomy, it would appear as if the entire maxilla has moved anteriorly. In two-jaw cases, determining the symmetry of the maxillary dental arch in the mediolateral plane with model surgery alone is extremely difficult and can lead to iatrogenic skewing of the jaws (Ellis 1990): it could be improved by the use of 3D virtual surgeries that relate the skeletal components to the dentition.

Conventionally, analysis of the 2D radiographs must be transferred to the models through an estimation of relation of the cast to the lateral headfilm. However, evaluating two-dimensional radiographs has its own set of limitations, such as effects of projection, patient position, and identification of landmarks.

Landmark Error

Landmark identification error is an important factor in cephalometric analysis whether it is conducted in two-dimensions or three-dimensions. A classic study on landmark identification was conducted by Baumrind *et al.,* who reported the distribution of landmark selection by orthodontic residents (Baumrind and Frantz 1971). Baumrind *et al.,* concluded that errors in

landmark identification are too great to ignore and the magnitude of error varies greatly from landmark to landmark (Baumrind and Frantz 1971). Other studies have also found there to be errors in landmark identification that are considerable(Richardson 1966; Stabrun and Danielsen 1982; Haynes and Chau 1993; Tng, Chan et al. 1994; Trpkova, Major et al. 1997; Perillo, Beideman et al. 2000) Also, errors are larger when identifying landmarks on curves with larger radii (Baumrind and Frantz 1971), such as with soft tissue landmarks on the lips (Haynes and Chau 1993). A meta-analysis of 6 studies on landmark identification error concluded that errors in the x-axis of 0.59 mm and in the y-axis of 0.56 mm are "acceptable levels of accuracy" (Trpkova, Major et al. 1997).

In terms of three-dimensional landmark identification, De Oliveira *et al.,* (de Oliveira, Cevidanes et al. 2009) reported excellent intra- and inter-observer reliability in landmark identification in three-dimensions, with 76.6% of the landmarks identified having a mean difference 1mm. Lagravere *et al.,* (Lagravere, Low et al.), also reported high intra- and inter-examiner reliability for landmark identification, but with high means of error (0.1-4 mm in each dimension). The landmarks with greater error were associated with ill-defined 3D landmark definitions, curved surfaces, and landmarks located in areas of low density with poor visualization (Lagravere, Low et al.). One advantage in identifying landmarks in three dimensions is that patient orientation errors caused by improper alignment in the cephalostat are not an issue with CBCT imaging as the image can be oriented digitally after the scan. Also, compared to traditional cephalometric radiographs, CBCT images have no projection errors associated with magnification as the scans are 1:1 in size (Mah and Hatcher 2004). In addition, the image can be adjusted in many ways to facilitate location of the landmark, such as by rotating or clipping.

Superimposition

Assessment of the surgical outcomes requires a choice of stable reference landmarks or structures for superimposition. For assessing adult surgical patients, superimposing on structures that were not altered in surgery is sufficient. For growing patients, the superimposition region should include areas that have completed growth at an early age, such as the anterior wall of sella, anterior clinoid processes, planum sphenoidale, lesser wings of the sphenoid, and other areas of the anterior cranial base (Melsen 1974; Bjork and Skieller 1983).

The accuracy of superimposition is improved with increasing the number of landmarks included in the superimposition protocol (Gliddon, Xia et al. 2006). However, landmark identification in three-dimensions is problematic as it requires definitions of the landmark locations in all three planes of space, adds more error due to the additional dimension, and is complicated by requiring placement of landmarks on curved surfaces (Schlicher, Nielsen et al. ; Dean, Hans et al. 2000; de Oliveira, Cevidanes et al. 2009). Therefore, superimpositions should not rely on landmark identification.

Also, the superimposition technique used should not depend on the precision of segmentation of surface models, but rather the original scan should be used without segmentation (Carvalho Fde, Cevidanes et al.). In a prior study, Cevidanes *et al.,* (Cevidanes, Bailey et al. 2005) reported using surface models in the superimposition protocol, and the error was found to be 0.77 mm. Now, software tools that utilize a superimposition algorithm based on the relative densities of voxels allow for superimpositions with an accuracy at the subvoxel level (Cevidanes, Styner et al. 2006).

Cevidanes *et al.,* demonstrated that superimposition on the anterior cranial fossa is a valid and reproducible means for assessment of treatment outcomes for growing subjects with error less than 0.5 mm (Cevidanes, Heymann et al. 2009). Cevidanes *et al.,* stated that the

superimposition protocol used "the best anatomic fit of anterior cranial base structures that have completed growth by age 7: anterior wall of sella, anterior clinoid processes, planum sphenoidale, lesser wings of the sphenoid, superior aspect of ethmoid and cribriform plate, cortical ridges on the medial and superior surfaces of the orbital roofs, and inner cortical layer of the frontal bones." An example figure showing the region of superimposition is shown in Figure 2. However, this technique has some limitations as Cevidanes *et al.,* reported it to be too time-consuming and computing intensive to use routinely. Also, the protocol requires reformatting the scans to a voxel size of 0.5 mm^3 because smaller slice thicknesses would increase the size of the files and require more computational power and user interaction time (Cevidanes, Styner et al. 2006).

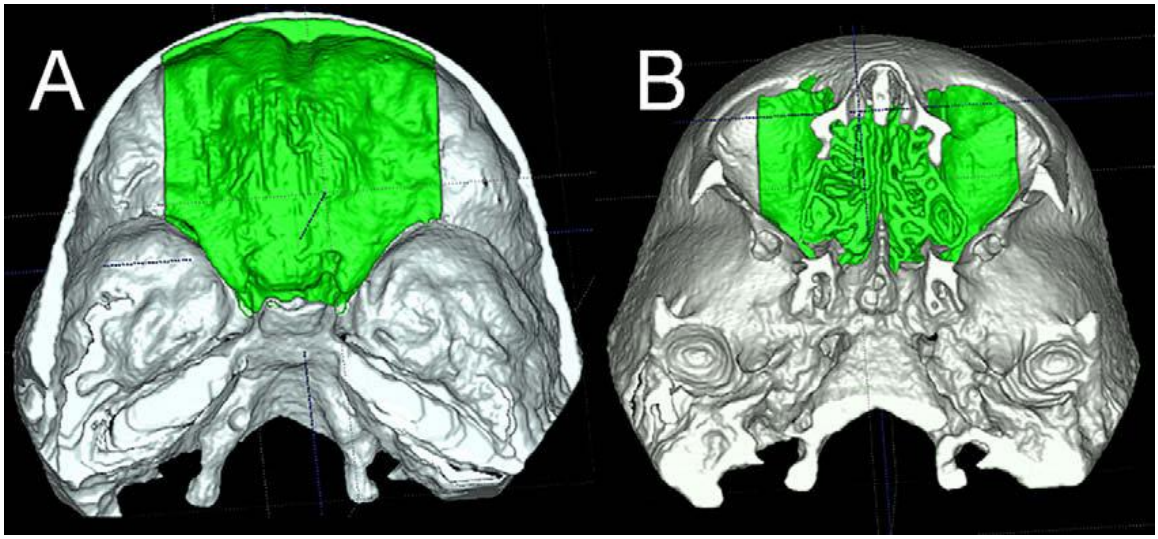

Figure 2. Region used for superimposition in growing subjects (Cevidanes, Heymann et al. 2009) A**, Superior view;** B**, inferior view.**

Xia *et al.,* also reported on the accuracy of their superimposition technique which was based on a best fit of surface models. The mean differences between two landmarks were found to be less than 0.1 mm with a standard deviation of 0.2 mm (Xia, Gateno et al. 2007).

Virtual Surgery Simulation

Three-dimensional image processing can enhance planning of surgical treatments and improve outcomes (Maki, Inou et al. 2003). This technique can overcome many of the limitations associated with model surgery, most notably the simultaneous access to information on the patient's skeletal anatomy during the planning process (Swennen, Mollemans et al. 2009; Swennen, Mommaerts et al. 2009). Swennen stated that "3D virtual treatment planning allows one to focus more on 3D facial harmonization, rather than on the facial profile (Swennen, Mollemans et al. 2009)."

Additional advantages of virtual surgical simulation have been reported (Swennen, Mollemans et al. 2009) including the accurate assessment of the upper dental midline to the facial midline, of the chin position and anatomy, and accurate assessment of the occlusal plane cant, which has implications on the paranasal area, gonial angles, lower mandibular borders, and chin. Also, during the virtual surgery, the amount of mandibular movement can be accurately measured on both sides since the proximal fragments remain stationary relative to the distal segments unless otherwise desired. Additionally, multiple treatment plans can be virtually attempted and evaluated (Swennen, Mollemans et al. 2009).

It has been shown that orthognathic surgeries can be planned virtually utilizing any of a number of software applications (Xia, Ip et al. 2000; Meehan, Teschner et al. 2003; Sohmura, Hojo et al. 2004; Chapuis, Schramm et al. 2007; Swennen, Mollemans et al. 2009; Bell 2011). In 2000, Xia *et al.,* presented a virtual reality system for planning orthognathic surgery, the Computer Assisted Three-dimensional Virtual Osteotomy System (CAVOS) (Xia, Ip et al. 2000). They created a virtual reality environment in which to perform the surgeries and applied this technique to 10 patients. Performing the virtual simulation was found to be very time consuming and computing intensive. Meehan *et al.,* (Meehan, Teschner et al. 2003)

demonstrated the use of an experimental Craniofacial Surgery Planner for use in planning surgeries with the ability to estimate the soft tissue changes. In 2007, Xia *et al.,* (Xia, Gateno et al. 2007) and Gateno *et al.,* (Gateno, Xia et al. 2007) described a computer-aided surgical simulation (CASS) for use in treatment planning of complex craniomaxillofacial deformities. Bell (Bell 2011) described many software programs available for applications in craniofacial surgery, orthognathic surgery, head and neck reconstructive surgery, and dental implantology, including, but not limited to Amira (Berlin, Germany), Analyze (AnalyzeDirect, Lenexa, Ann Arbor, MI), Intellect Cranial Navigation System (Stryker, Freiburg, Germany), InvivoDental (Anatomage, San Jose, CA), iPlan (BrainLab, Westchester, IL), Maxilim (Medicim, Bruges, Belgium), MIMICS, Surgicase CMF, and Simplant OMS (Materialise, Leuven, Belgium), Voxim (IVS Solutions, Chemnitz, Germany), and 3dMD (Atlanta, GA). Bell presented a series of cases in which SimPlant OMS (Materalize, Leuven, Belgium) was utilized for virtual surgical planning and in splint fabrication. At the conclusion of the article, Bell states "computer-based surgical simulation has the potential to completely replace the reference standard of analytical model surgery with plaster casts as the preferred method of treatment planning for '2-jaw' orthognathic surgery cases, although *additional study evaluating the accuracy is necessary*. In addition, studies that provide outcomes data and cost-benefit analyses for each of these indications are lacking and necessary before widespread adaptation of these techniques" (Bell 2011).

The clinical accuracy of 3D virtual surgical planning methods has sparsely been reported. Chapuis *et al.,* (Chapuis, Schramm et al. 2007) reported on the use of the craniomaxillofacial (CMF) application software (developed at the M.E. Müller Institute for Surgical Technology and Biomechanics, University of Bern, Switzerland) in a single case which showed a median prediction accuracy of 0.9 mm based on a color map. However, an area of the color map had a

"realistic maximum error" of 2.9 mm given by the 95th percentile of the color map distance values.

Xia *et al.,* evaluated the accuracy of the CASS planning method on patients with complex craniomaxillofacial deformities (Xia, Gateno et al. 2007). Five patient simulations were performed and splints generated. The criteria used in their study were derived from studies that evaluated the accuracy of planning methods in orthognathic surgery using 2D cephalograms. Differences of prediction to outcomes of less than 2 mm and angular differences of less than 4 degrees were used to determine accuracy. Previous studies based on lateral headfilms have determined that a difference of less than 2 mm in linear measurement or 4° in rotation is not likely to be clinically significant. As cited previously, Donatsky *et al.,* (Donatsky, Bjorn-Jorgensen et al. 1997) reported the accuracy between planned and actual outcomes to be approximately 2 mm. Jacobson and Sarver (Jacobson and Sarver 2002) reported that 80% of actual postoperative outcomes fell within 2 mm of the prediction. Padwa *et al.,* (Padwa, Kaiser et al. 1997) reported that an occlusal cant of less than 4° was clinically insignificant. Xia *et al.,* found the median differences between planned and actual postoperative outcomes to be 0.9 mm and 1.7 degrees (Xia, Gateno et al. 2007).

In addition, Tucker *et al.,* in 2010, validated the ability of virtual orthognathic surgery using craniomaxillofacial (CMF) application software to recreate orthognathic surgery hard tissue movements (Tucker, Cevidanes et al.). This study used the actual postsurgical positions of the osteotomies to recreate simulations of Le Fort I maxillary advancements and mandibular BSSO setbacks (1- and 2-jaw surgeries). The error in placement of the virtual models was found to be within 0.5 mm, which is within the voxel size of the scans. The level of accuracy that can be achieved without using the postsurgical result as a guide for the placement of the virtual models remains to be determined.

Purpose

The purpose of this study is to evaluate the accuracy of 3D virtual orthognathic surgery simulation in single jaw surgery performed by a single surgeon using a commercially available software package, InVivoDental v5.1 (Anatomage, San Jose, CA USA).

Specific Aims

The specific aims are:

- Part 1: Determine the most reproducible orientation method for CBCT scans of the head in order to identify a standard orientation to be used with multiple scans for use in 3D cephalometry, and to be able to compare two time points without the need for superimposition. (NOTE: This aim was initially planned because the superimposition tools identified for use in the project had a limited set of tools for the analysis.)

- Part 2: Determine the feasibility of using virtual orthognathic surgery and identify limitations

    - Compare pre-surgical prediction with post-surgical result via 3D superimposition of scans, and measure differences in prediction vs. result

    - Compare accuracy of predictions between maxillary and mandibular single jaw surgeries

Hypothesis

Three-dimensional orthognathic surgical predictions developed from presurgical CBCT scans are an accurate means to predict surgical outcomes, as assessed by comparison of prediction to final postsurgical outcomes.

METHODS AND MATERIALS

Subjects

Part 1: Orientation Protocol Study

The sample for the initial study to examine the reproducibility of orienting the same scan using different protocols included CBCT data of 5 adult patients taken from the UCSF database of CBCT scans. The sample consisted of 4 males and 1 female with the average age of 30.2 years $\pm$ 1.1 yr SD.

Part 2: Virtual 3D Orthognathic Treatment Simulation Accuracy

A collection of records from 19 of Dr Janice Lee's patients (mean age 24.5 yrs; ranging from 15-44 yr), who have previously undergone orthognathic surgery involving one jaw. The records included CBCT scans taken within 6 weeks prior to surgery and 6 weeks postsurgery, chart notes, and photographs. Patients were excluded if they had severe craniofacial anomalies that altered the typical morphology of skeletal or dental structures, or if the scans did not include all landmarks used in the study. Table 1 shows the randomized ID, age/sex and surgical movements for each of the patients.

Patient	Pt ID #	Age	Gender	Surgical notes
Mn1	0.029	20	F	7mm adv
Mn2	0.027	31	F	7mm adv
Mn3	0.335	27	F	7mm adv
Mn4	0.412	33	F	5mm adv
Mn5	0.993	19	F	-4mm setback / 3mm rotation left
Mn6	0.652	37	M	?mm setback
Mn7	0.713	44	F	6mm adv
Mn8	0.824	38	F	6mm adv
Mn9	0.916	17	F	9mm adv / 1mm closure
Mn10	0.825	18	F	10mm adv
Mx1	0.026	16	F	5mm adv
Mx2	0.356	19	F	4mm adv/3mm rot left/ 1mm ant lengthen
Mx3	0.451	26	M	6mm adv
Mx4	0.560	18	F	5mm adv / 3mm ant lengthen
Mx5	0.589	18	F	6mm adv
Mx6	0.636	15	F	4mm adv / 4mm ant lengthen
Mx7	0.675	28	F	5mm ant superior / 3mm post superior
Mx8	0.635	21	M	5mm adv / 1mm rot right
Mx9	0.599	21	F	5mm adv

Table 1. Subjects for Retrospective Study

CBCT Protocol

The cone beam CT scans were taken with the Hitachi CB MercuRay (Hitachi Medico Technology, Tokyo, Japan) with the same setting and techniques used for each scan (15 mA, 120 kVp). A total of four operators took the scans following the same protocol. With the patient sitting upright, a rotating source/detector gantry captured a volumetric image of the patient's head. A 10-second scan acquired 512 images in a 12'' diameter spherical volume with 0.2-0.376

mm^3 voxels in high-resolution mode and 12 bits/voxel (2^{12} = 4096 shades of gray). The version of the system used in this study has a scalable 12'' CCD (coupled current detector) detector that can be set in several fields of view (FOV) modes. In order to capture anatomy critical for orthodontic diagnosis and treatment planning, the 12-inch receiver was used. The resulting Digital Imaging and Communication in Medicine (DICOM) datasets were made anonymous and imported to InvivoDental Version 5.0 beta (Anatomage, San Jose, CA).

Landmarks

Definitions for three-dimensional anatomic landmarks were determined by a review of the current literature and through discussion with UCSF faculty members in the Division of Orthodontics (Schlicher, Nielsen et al. ; Solow 1966; Swennen, Schutyser et al. 2005). The final definitions used for the landmarks in the orientation study are presented in Table 2.

Landmark	Definition
Sella	Geometric center of the hypophyseal fossa
Sella Prime	The point of greatest convexity on the most superior anterior portion of the hypophyseal fossa equidistant to the anterior clinoid processes
Nasion	The most anterior and median point along the frontonasal suture.
Frontozygomaxillary point (Right & Left)	The most medial and anterior point of each frontomaxillary suture at the level of the lateral orbital rim (Swennen, Schutyser et al. 2005)
Opisthion	The most inferior point on the anterior border of the foramen magnum; the most posterior-inferior point on the clivus. (Solow 1966)
Clivus	The most inferior point of the shallow depression behind the dorsum sella
Crista Galli	The most superior point of the median ridge projecting from the cribiform plate
Porion (Right & Left)	The most superior point of the external acoustic meatus located laterally at the point when the meatus is entirely encircled in bone.
Orbitale (Right & Left)	The deepest point of the infraorbital margin

Table 2. Three-dimensional landmark definitions used for the orientation protocols.

Part 1: Orientation Protocol

Four orientation methods were evaluated to determine which is the most reproducible with the least variation between time points. Five scans were utilized, each of which had a set of 8 landmarks with x, y, and z coordinates: A point, anterior nasal spine, B point, pogonion, right gonial angle, LR6 mesiobuccal cusp, UR1 root, and UR1 tip. Each scan was oriented at 3 time points, separated by 3-4 weeks, using the 4 different orientation methods. A second rater repeated the study in order to determine inter-rater reliability. The data consisted of 8 x, y, and z coordinates on 5 scans with 4 different orientation methods completed at 3 time points by two raters saved in multiple Excel files (Microsoft, Redmond, WA). Orientation 3 was completed

utilizing the planar views, as opposed to the other three orientations which were completed by picking landmarks on the volumetric views with the 3D cephalometry tool.

Orientation 1: Modified Frankfort Horizontal

- Origin: Sella Prime (Figure 3)
- Horizontal plane (modified 3D Frankfort based on 3 points: both orbitales and right porion
- Midsagittal plane: perpendicular to horizontal plane including a line from center of sella to nasion
- Frontal plane: dropped from sella prime perpendicular to the other two planes

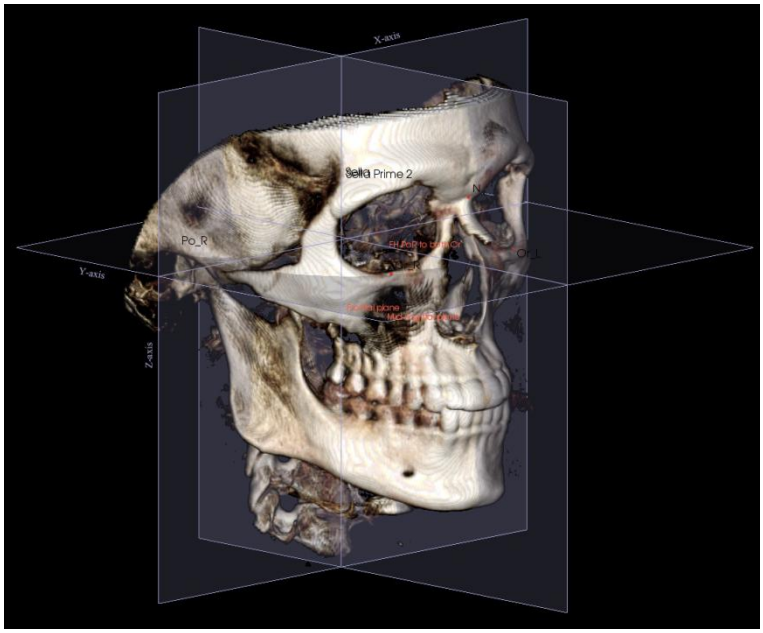

Figure 3. Orientation 1: Modified Frankfort Horizontal

Orientation 2: Anatomage Default

- Origin: Nasion (Figure 4)
- Midsagittal plane: Perpendicular plane to a line connecting right and left porions through nasion
- Horizontal plane: 3D Frankfort using right porion and right orbitale, and perpendicular to midsagittal plane
- Frontal plane: dropped from nasion perpendicular to other two planes

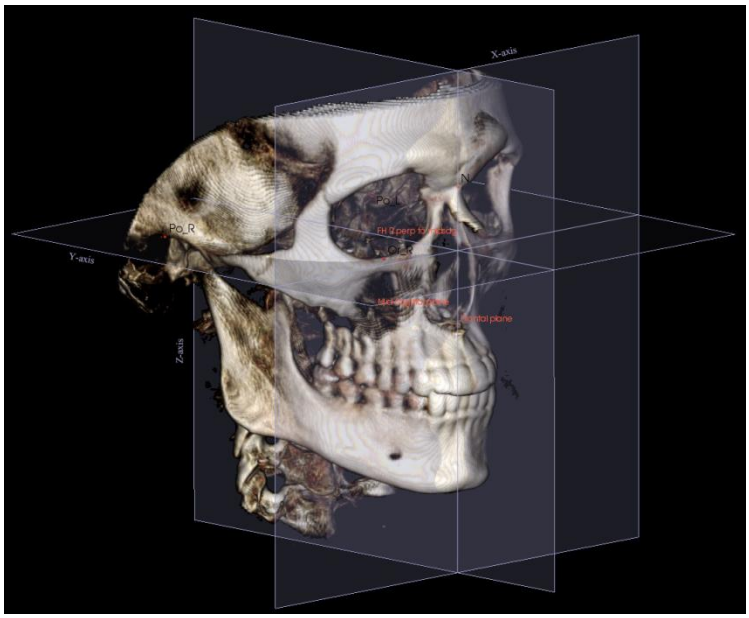

Figure 4. Orientation 2: Anatomage Default

Orientation 3: UCSF Planar View

- Origin: Sella Prime (Figure 5)
- Horizontal plane – 2 pts: sella and nasion AND parallel to a line connecting Fz sutures
- Midsagittal plane – 2 pts: opisthion and crista galli AND perpendicular to horizontal plane

- Frontal plane – origin pt (sella prime) AND perpendicular to both horizontal and midsagittal planes
- Created in section views
    - Coronal: Fz –Fz
    - Axial : opisthion to crista galli
    - Sagittal: S-N

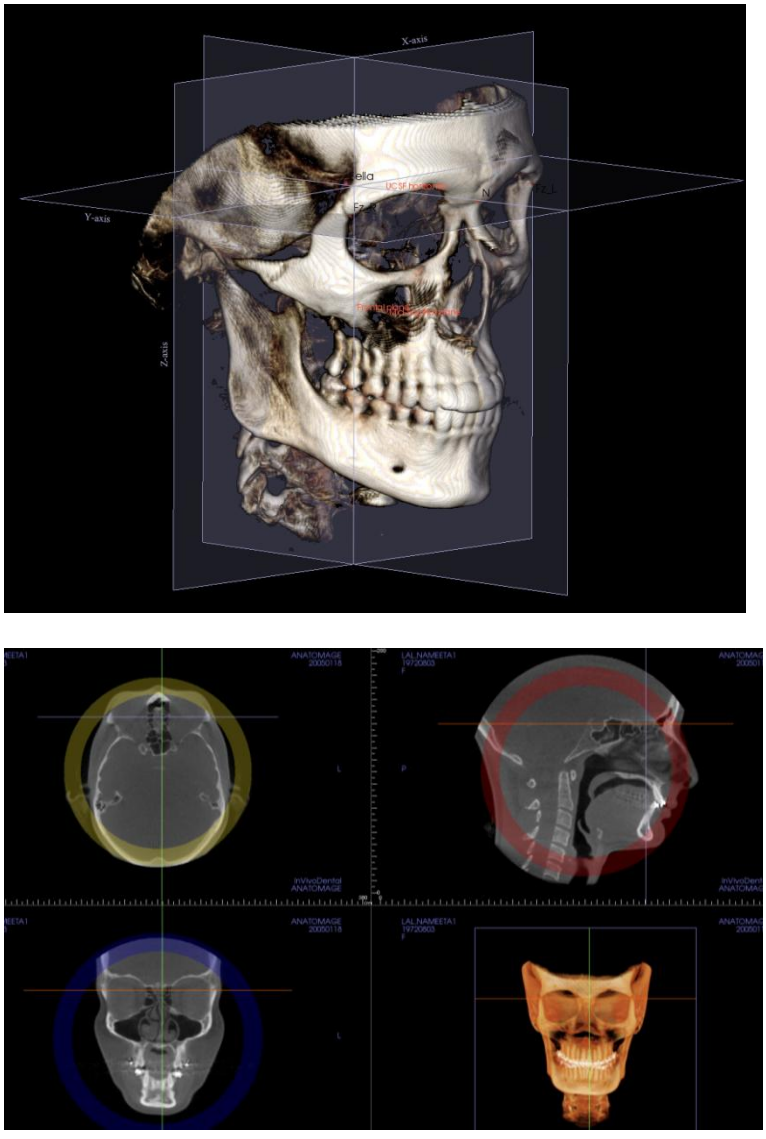

Figure 5. Orientation 3: UCSF Planar View. Top) Volume rendering of a patient oriented to Orientation 3. Bottom) Planar views for completing the orientation protocol.

Orientation 4: Nasion-Frontozygomatic suture-based Orientation (NFZ Based Orientation)

- Origin: Nasion (Figure 6)
- Horizontal plane: defined by 3 points: nasion and both frontozygomatic sutures
- Midsagittal plane: parallel to crista galli-clivus line passing through nasion and perpendicular to horizontal plane
- Frontal plane: perpendicular to the other 2 planes through nasion

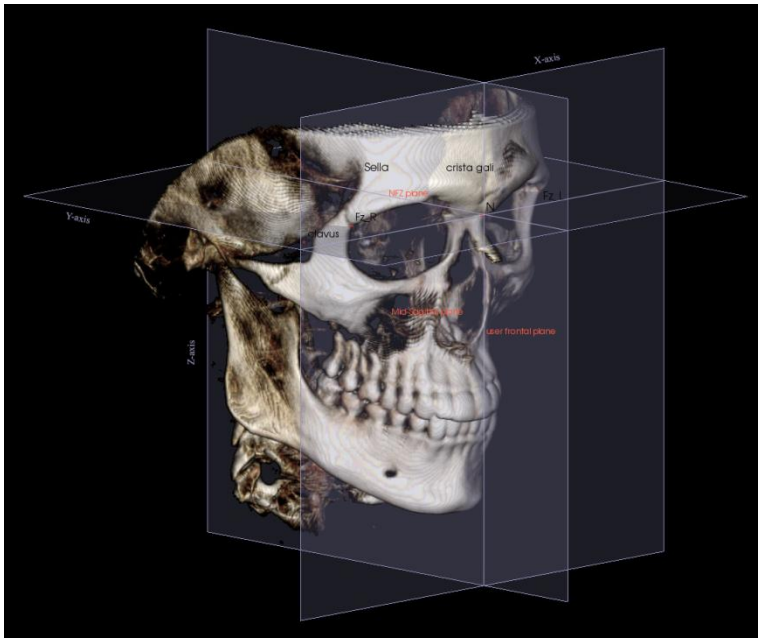

Figure 6. Orientation 4: NFZ Based Orientation

Protocol for Orientations

See Appendix A "Orientation Protocol"

Statistical Analysis

The mean and standard deviation for each time point for each landmark specific to the subject and orientation method were determined. The standard deviations for each landmark for all five subjects were then averaged, giving the average precision for each orientation

method. This average standard deviation was then compared across the four orientation methods to determine the most precise method of orientation.

A mixed effects model was used to evaluate the difference between orientation methods to determine which methods were most reproducible. The outcome variables examined were the rotation size around each axis (yaw, pitch, and roll) compared to the mean for that time point, and the residual sum of squares, which is given by the following formula:

> 1/(8*3) SUM (SUM (SQRT((xij-x.j)^2 +(yij-y.j)^2+(zij-z.j)^2)))) where i is time point; j is landmark j=1-8 i=1-3
>
> where e.g. x.j = the mean of the x coordinates across the 3 time points for landmark j

The residual sum of squares is a measure of the discrepancy between the data and an estimation model. A small RSS indicates a tight fit of the model to the data. The predictors to be assessed were the effect of the rater and the orientation method used.

Part 2: Virtual 3D Orthognathic Treatment Simulation Accuracy

A series of steps were followed to compare the predicted result to the actual outcome.

Figure 7. Flowchart of the methods used to compare the virtual predictions to the postsurgical outcome

Protocol for Segmentation

The following protocol was followed.

1. Upload anonymized presurgical CBCT scan data sets to Anatomage for segmentation into maxillary and mandibular segments, known as Anatomodels. (NOTE: In a trial, the segmentation was attempted using the Medical Design Studio tool of the InvivoDental software package but with little success due to the difficulty in separating the occlusal anatomy of the upper and lower dentition from scans taken with patient's teeth in occlusion.)

2. Download Anatomodels and open in InvivoDental 5.0 beta.

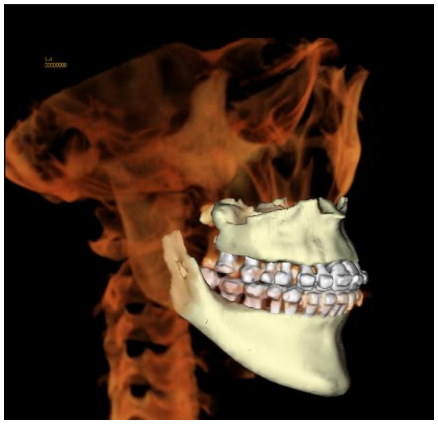

Figure 8. Example of a volumetric view with segmented maxilla and mandible (Anatomodels).

3. In the ModelView tab, the user begins the process of performing the planned surgery based on the treatment plan and measurements recorded in the patient chart. Actual distances moved are automatically calculated as the user manipulates models in space on the program as a guide.

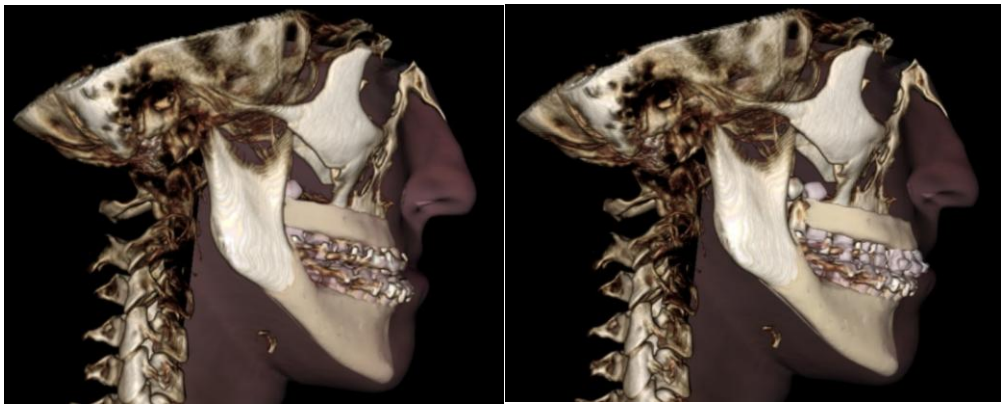

Figure 9. A) Presurgical scan with segmentation to show an example of a LeFort I maxillary advancement simulation. B) Simulation of maxillary LeFort I advancement

Protocol for Surgical Simulations

1. The user sets the color of maxillary dentition to orange and keeps the lower dentition as white, to be able to easily differentiate maxillary from mandibular dentition when setting up the occlusion. Completed by clicking Settings button in ModelView for each segmented tooth in the maxilla.

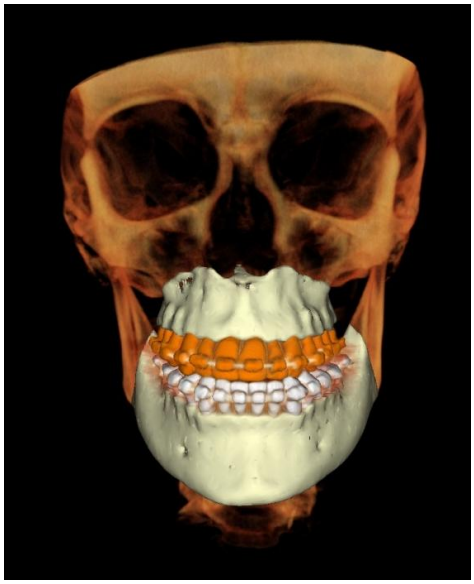

Figure 10. Frontal view of Anatomodels demonstrating the orange coloration of the maxillary dentition

2. Open Simulation dropdown menu and add new simulation title corresponding to the surgery to be planned, such as “Max Adv 5mm, Rotation 3mm Left”

3. To highlight the jaw to be moved, slide simulation slider to the leftmost position (indicating final position), an orientation widget associated with that object will become visible. Orient this widget according to the vector of surgical movements to occur. For example, in the case of a maxillary surgery where the occlusal plane of the maxilla will not be altered, set the horizontal and sagittal planes to be level to the existing occlusal plane.

4. After the virtual gross surgical movements have been completed, begin to set up the occlusion properly.

    a. Set midline to desired location

    b. Set overbite and overjet as determined by treatment goal

    c. Check overbite by sagittal clipping; increase brightness to ensure that linear measurement is taken on SD surface instead of 3D

    d. Ensure that physics are obeyed by checking penetration of model into stationary model. This is where having a separate color for the opposing dentition becomes very useful.

    e. Once anterior goals are achieved virtually, move orientation widget to the contact point of the upper and lower incisors and adjust yaw and roll for occlusal contacts posteriorly. (NOTE: with the resolution from a CBCT alone, the inferior occlusal anatomy of the posteriors makes this very challenging.)

f. Use coronal clipping and axial clipping to ensure that the contacts are even on both sides. It is recommended to adjust the plane of the axial clipping by reorienting the horizontal plane of the scan to match with occlusal plane. This allows for easier visualization of the posterior contacts when clipping axially.

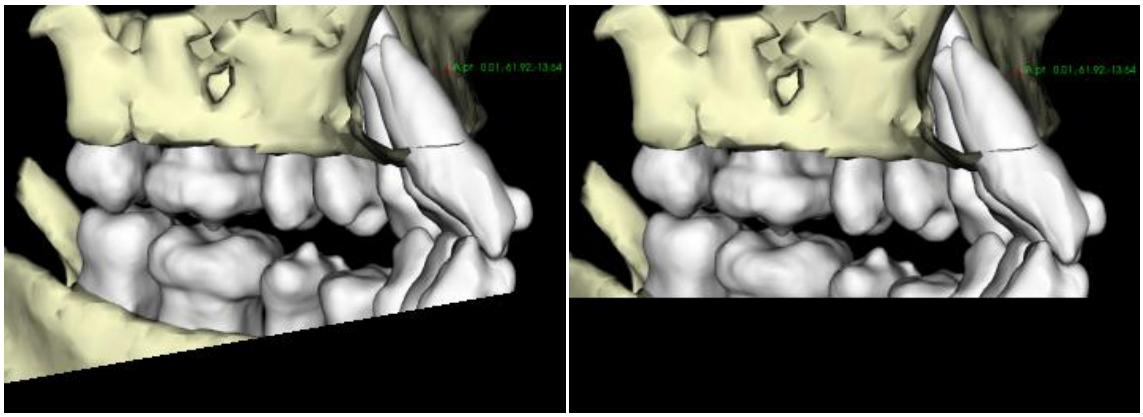

Figure 11. Sagittal view of Anatomodels demonstrating that clipping parallel to the occlusal plane allows for better visualization through the teeth to evaluate for heavy posterior contacts

Special Considerations for Maxillary Surgeries

In maxillary surgeries, the mandible needs to be autorotated around the estimated hinge axes. In order to simulate this, the orientation widget for the mandible needs to be moved so that the x axis runs through the hinge axis of each condyle. The mandible can then be rotated open or closed as needed.

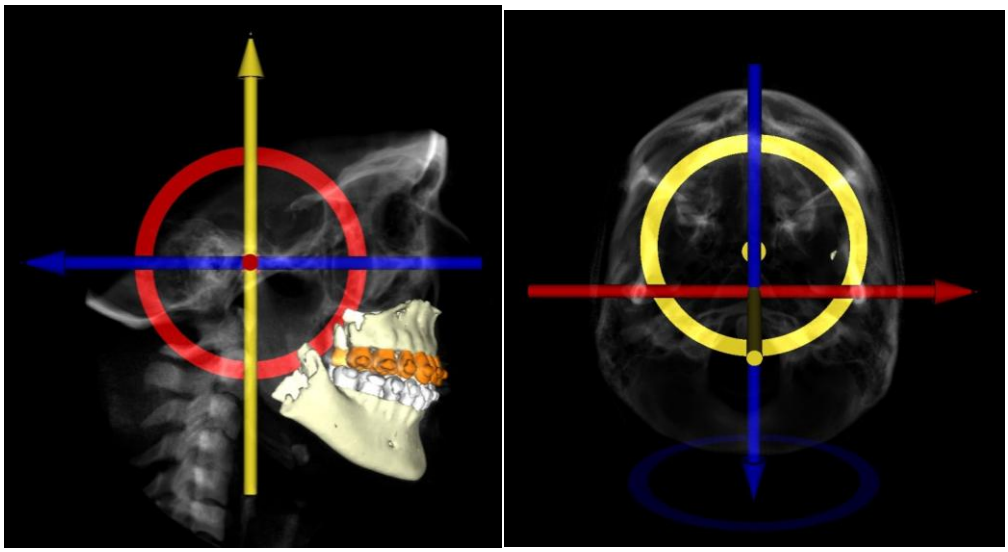

Figure 12. A) Sagittal view demonstrating the placement of the widget through the condylar hinge axis. B) Axial view demonstrating the placement of the widget through the condylar hinge axis. Preset view of 'X-ray' shown here.

Analysis of Surgical Simulations

Superimposition Protocol: superimpose surgical prediction model on actual postsurgical CBCT scan

1. Open presurgical scan with simulation, and orient to Orientation 1 protocol
2. Open Superimposition tool, choose "Import New Volume" and open postsurgical scan
3. Begin superimposition protocol:
    a. Identify at least 4 landmarks on both scans for initial superimposition. If available, use frontozygomatic sutures, nasion, and at least one point posteriorly which is easily identifiable, such as a projection on the mastoid, an extension of the lambdoid suture, or a foramen.

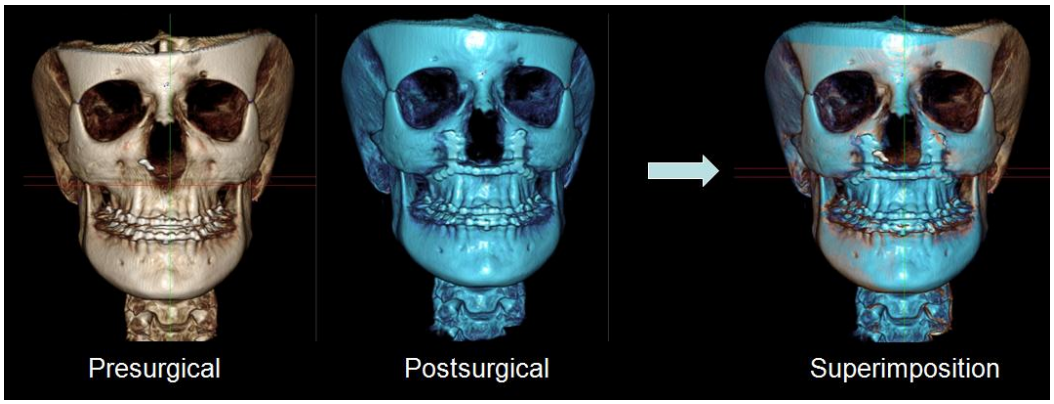

Figure 13. Result of 5 pt registration. Postsurgical volume shown in blue. Postsurgical model too far to the patient's right: requires slight manual adjustment

b. Manually adjust as needed for closest approximation of superimposition of cranial base structures. Using the toggle between original and superimposed volumes to identify what adjustments need to be made. Then the superimposition is saved.

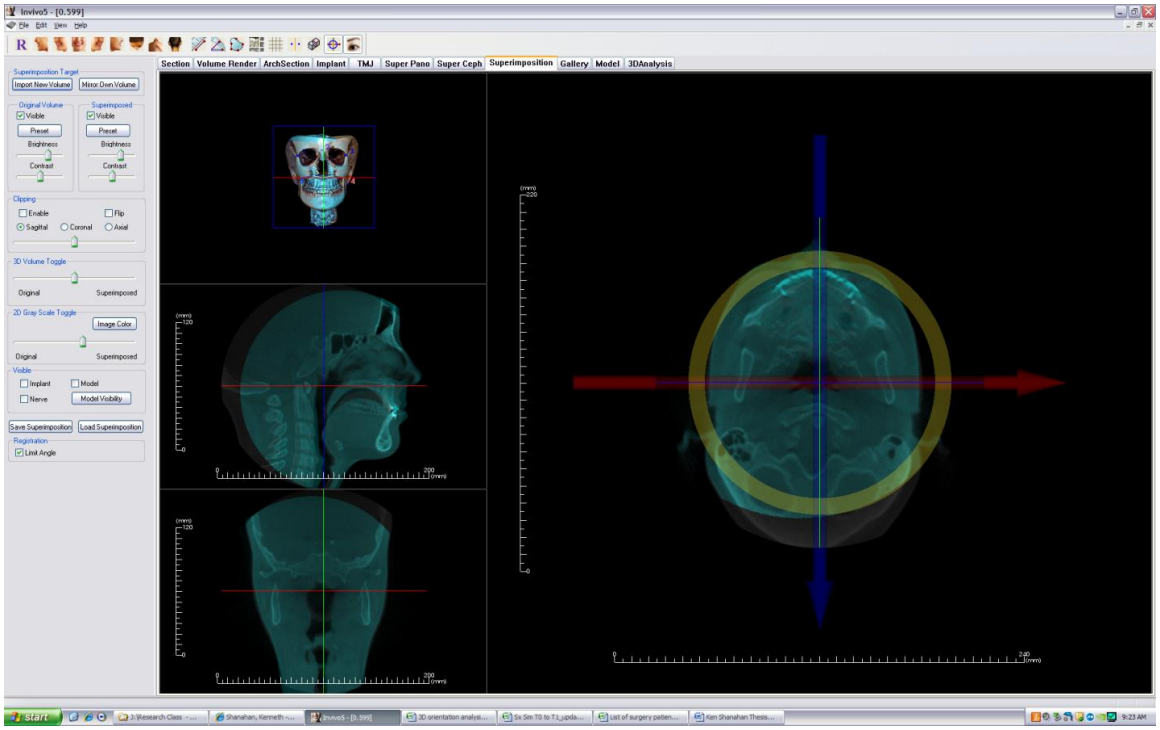

Figure 14. Manual adjustment of the superimposition of the postsurgical scan (shown in blue). The presurgical scan is held constant while the postsurgical scan is moved relative to the presurgical scan and its corresponding coordinate system.

c. Superimpose by volume (50x50x30mm) centered at anterior sella, including anterior cranial base structures such as anterior clinoid processes, planum sphenoidale, lesser and most of the greater wings of the sphenoid, and others. The volume is adjusted as necessary to avoid any areas that showed changes between CBCT scan time points, such as postsurgical sinusitis.

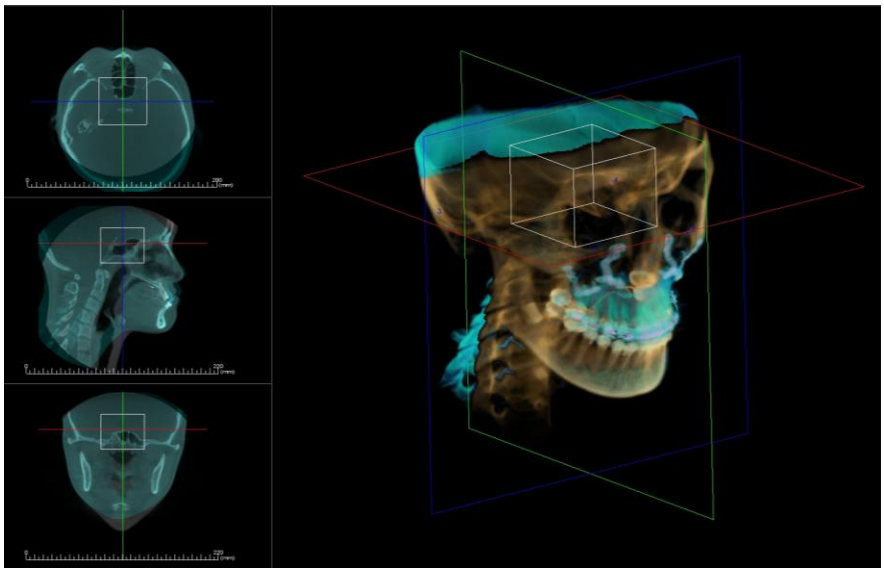

Figure 15. Example demonstrating the placement of the volume to be used for the superimposition, centered at anterior sella.

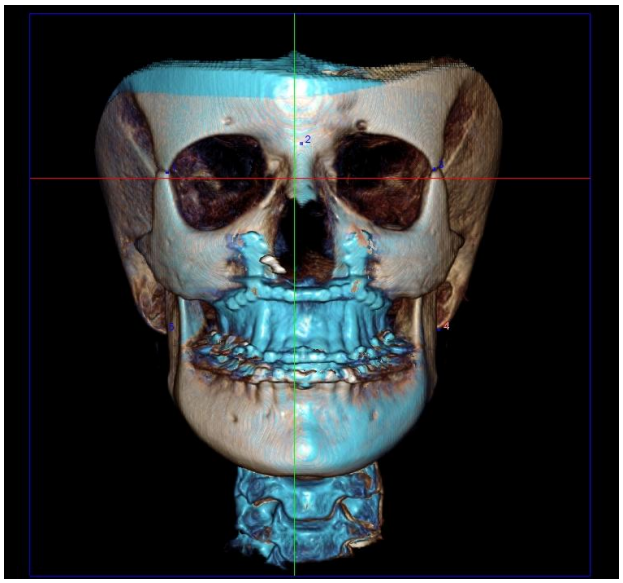

Figure 16. Completed superimposition by volume of interest.

Superimposition Reliability

Prior to using the volume of interest automated superimposition tool, it was necessary to test the accuracy of this technique. A CBCT scan of a dry skull with 2 mm diameter metallic markers, shown in white in Figure 17 and Figure 18, was duplicated and randomly reoriented. The scan to be superimposed was manually reoriented to match the original scan as close as possible. The volume of interest used to base the superimposition was set to a 50x50x30 volume centered at anterior sella, and the automated superimposition was completed. At this point, eight of the metallic landmarks were identified digitally on the original scan with the superimposed scan hidden, and the 3D coordinates were recorded in an Excel spreadsheet. Then, the same eight landmarks were identified on the superimposition scan with the original scan hidden and recorded. The landmarks used were A point, ANS, B point, right and left gonion, LR6 mesiobuccal cusp, pogonion, and the U1 root apex. In order to minimize the influence of landmark identification error, this landmark identification process was repeated three times in one sitting. The mean for each landmark was determined and the difference between the means of the landmarks was measured. The volume superimposition was repeated two times, for a total of three time points.

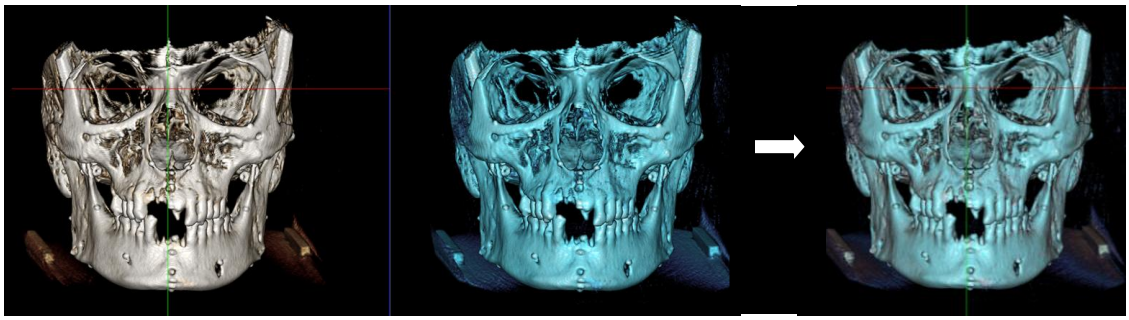

Figure 17. Volumetric views of original scan (white) and superimposition scan (blue) and resulting superimposition. Landmarks were chosen on each scan separately and 3D coordinates recorded.

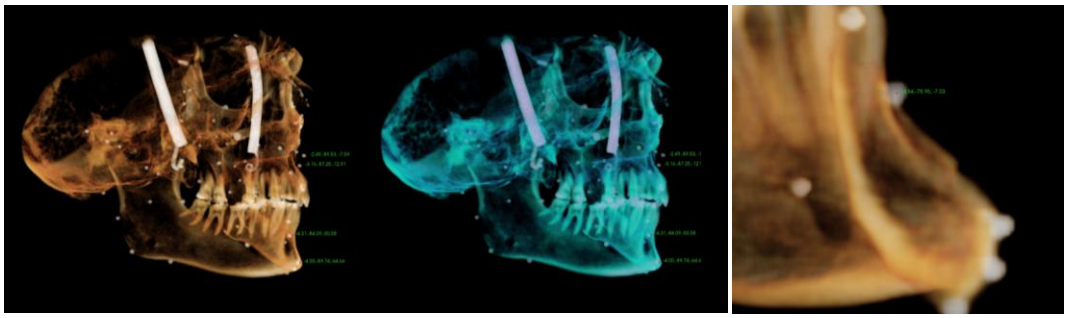

Figure 18. Volumetric views of the dry skulls with metallic markers visible, original scan (white), blue scan (superimposition scan), and a close-up view of the center of the marker representing B point digitally identified.

Quantify the Differences between Prediction and Postsurgical Outcome

In order to quantify the difference between the prediction and the postsurgical scans, landmarks were identified on each at the mesiobuccal cusps of the first molars and the contact point of the central incisors, as described by Xia *et al.,* (Xia, Gateno et al. 2007). These landmarks allowed for the jaws to be represented as triangular planes from which centroids could be used to measure differences horizontally, vertically, and sagittally, as well as the difference in rotation around the three axes: pitch, yaw, and roll.

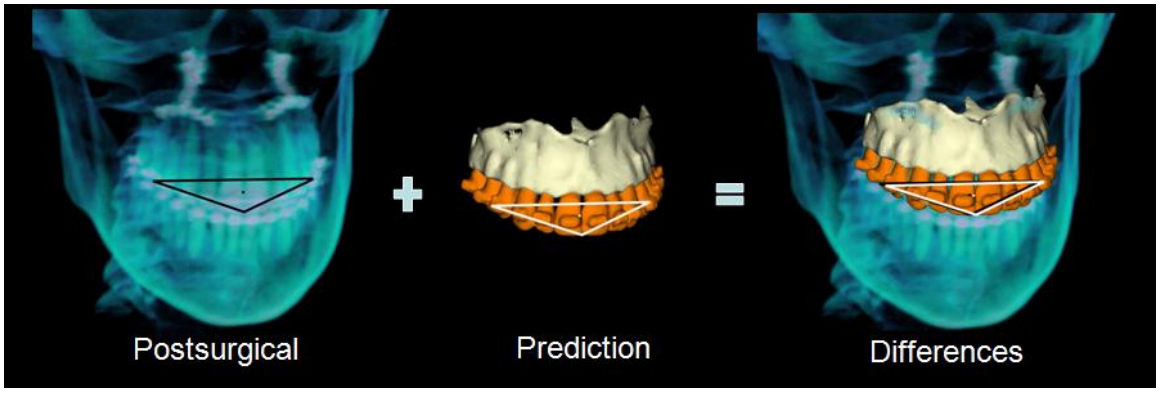

Figure 19. Example of a maxillary surgery in which landmarks were identified on the mesiobuccal cusps of the maxillary molars and at the contact point of the central incisors. The landmarks were identified on the postsurgical scan as well as the prediction, and connected by three lines to create a triangular plane. The differences in position of these planes could then be analyzed as well as the difference in rotations.

The process involved the following procedures.

1. Open Model view, place landmarks at the contact point of the central incisors, the most occlusal point on the mesiobuccal cusp of the right and left first molars for the maxilla in maxillary surgeries and the mandible in mandibular surgeries, as described by Xia *et al.,* (Xia, Gateno et al. 2007).

    a. Begin with picking the landmarks on the models with the rest of the volumes hidden for T0, and repeat for the simulation end point (TP).

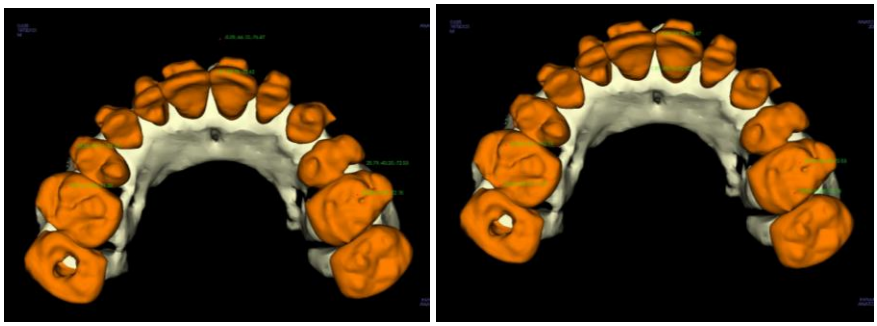

Figure 20. A) Model of maxilla with volumes hidden and landmarks identified. B) Prediction of maxilla position (maxillary advancement and rotation) with landmarks chosen to duplicate the position of the landmarks in T0. Accomplished by switching between views of T0 and view of TP to ensure landmarks are in the same location relative to the model.

    b. Make volume visible (ensure that the volume is set to similar brightness as the superimposed volume, and the preset is set to "Teeth"). Hide model from T0, using frontal and sagittal views with clipping to midline, add a new landmark over the current landmark from T0 model. Repeat this step for the MB cusps of the first molars in conjunction with axial clipping of the volume. View from the occlusal when picking the T0 landmarks; then view from sagittal to ensure that the landmark is on the occlusal surface of the molar and did not penetrate the molar.

(NOTE: This step is necessary to determine the adjustment that will be needed to be applied to the TP landmarks compared to the post surgical scans, as the segmentations slightly overestimate the size of the crowns of the teeth.)

c. Record landmarks by creating a report created from the "Volume Renderer" tab, and transfer to Excel document for recording results. Next, delete TP landmarks, so as not to bias the landmark identification of the post surgical result.

d. View postsurgical volume and identify the landmarks as in T0. Record.

Quantify Differences

The sets of three landmarks allowed for the jaws to be represented as triangular planes from which centroids could be determined which were compared to measure linear differences horizontally, vertically, and sagittally. In order to calculate the degree of difference in rotation around the three axes (pitch, yaw, and roll), linear regression was performed to determine the slope for each time point, and then the difference in slopes was calculated. For example, to determine the rotation around the Z-axis, or yaw, the z-axis was set to zero and only the x and y coordinates for the sets of three landmarks were considered (Figure 21). The slope of the linear regression of the 3 points at TP was then compared to the slope of the linear regression of the 3 points at T1. In Excel, the formula for determining the degree difference was:

=DEGREES(ATAN(SLOPE(3 sets of x, y coordinates for TP)))-DEGREES(ATAN(SLOPE(3 sets of x, y coordinates for T1)))

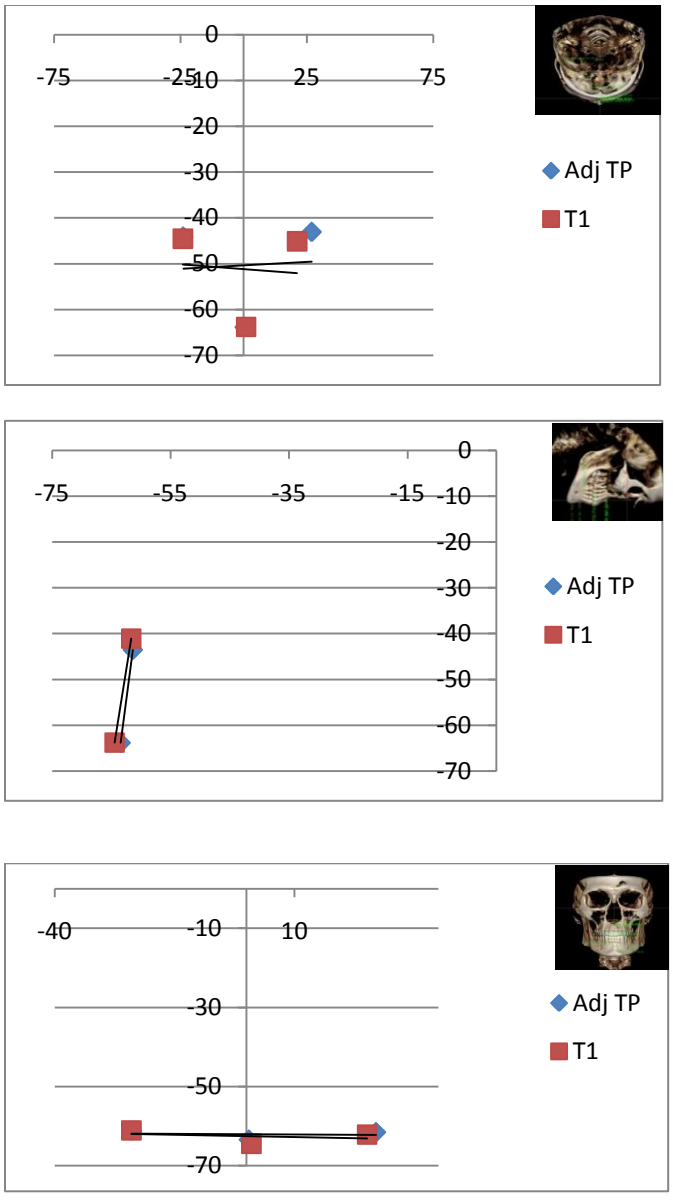

Figure 21. Plot of 3D coordinates from one surgery (Mn1). A) Z axis set to zero, and x, y coordinates plotted. Difference in yaw is 2.68° B) X axis set to zero, and y, z coordinates plotted. Difference in pitch is 1.31°. C) Y axis set to zero, and x, z coordinates plotted. Difference in roll is 0.95°. Graphics demonstrate the corresponding volumetric views for each plot.

Statistical Analysis

The magnitudes of the differences between prediction and postsurgical outcome centroids were determined as well as the standard deviations for each. Student t-tests were

performed to assess the effect of having a splint in place at postsurgical scan versus not having a splint. Student t-tests were performed to assess for differences in predictability of surgical outcome of maxilla versus mandible, as well as the right vs left side. A mixed effects model was used to determine the effect of the amount of surgical correction on the error in predictability.

Results

Part 1. Orientation Protocols

The outcome variables determined from the orientations portion of the project were the rotation size around each axis (yaw, pitch, and roll; Figure 22) compared to the mean for that time point, and the residual sum of squares, which is given by the following formula:

1/(8*3) SUM (SUM (SQRT((xij-x.j)^2 +(yij-y.j)^2+(zij-z.j)^2)))) where i is time point; j is landmark j=1-8 i=1-3

where e.g. x.j = the mean of the x coordinates across the 3 time points for landmark j

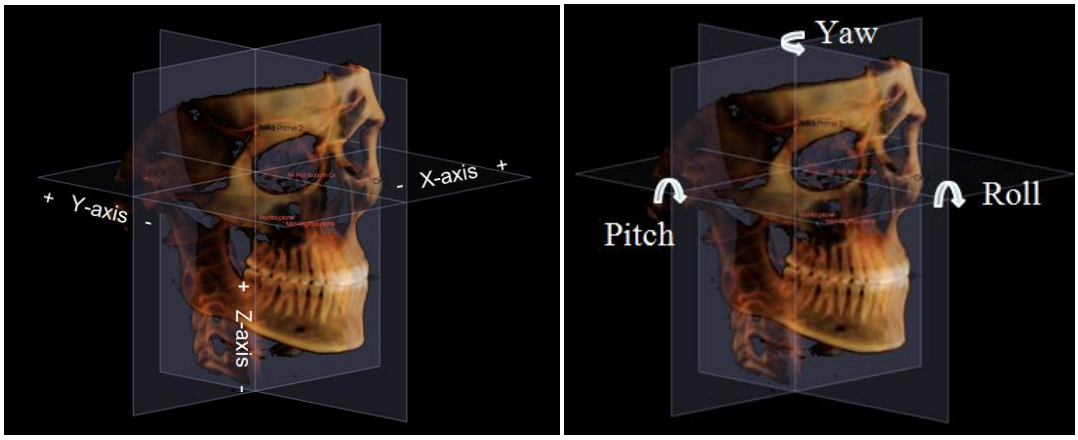

Figure 22. Orientation 1 coordinate system. A) Negative signs in this coordinate system correspond to right, anterior, and inferior directions. B) Volumetric view to demonstrate the direction of positive values in yaw, pitch and roll.

The residual sum of squares is a measure of the discrepancy between the data and an estimation model. A small RSS indicates a tight fit of the model to the data. The predictors to be assessed were the effect of the rater and the orientation method used.

A linear mixed effects model for single time point analysis was used as follows:

$$\text{distance}_{ijk} \sim \mu_i + r_j + o_k + \varepsilon_{ijk}$$

μ_i = random patient mean relative to rater 1, orientation 1. $i = 1,...,5$ (5 patients)

r_j = rater effect relative to rater 1: $j = 1,2.$ (2 raters)

o_k = orientation effect relative to orientation 1: $k = 1,...,4.$ (4 orientations)

where distance = RSS or angle of yaw, pitch, roll (Tables 3-4).

Patient	Orientation	RSS	Yaw (°)	Roll (°)	Pitch (°)
AS	1	0.60	0.20	0.16	0.20
EB	1	0.85	0.28	0.40	0.68
GC	1	0.44	0.15	0.55	0.19
JC	1	0.40	0.13	0.21	0.06
KS	1	0.53	0.18	0.24	0.18
AS	2	0.51	0.17	0.02	0.17
EB	2	0.89	0.30	0.40	0.31
GC	2	0.44	0.15	0.21	0.09
JC	2	0.68	0.23	0.69	0.43
KS	2	0.63	0.21	0.12	0.24
AS	3	0.74	0.25	0.29	0.28
EB	3	0.78	0.26	0.34	0.36
GC	3	0.57	0.19	0.27	0.18
JC	3	1.15	0.38	0.04	0.78
KS	3	0.89	0.30	0.17	0.54
AS	4	0.95	0.32	0.17	0.63
EB	4	1.38	0.46	0.15	0.97
GC	4	0.85	0.28	0.49	0.38
JC	4	2.02	0.67	0.46	1.43
KS	4	0.48	0.16	0.03	0.12

Table 3. Table of results of the orientation protocols for rater 1.

Patient	Orientation	RSS	Yaw (°)	Roll (°)	Pitch (°)
AS	1	1.10	0.37	0.29	0.45
EB	1	0.83	0.28	0.47	0.51
GC	1	1.06	0.35	0.23	0.17
JC	1	1.06	0.35	0.03	0.75
KS	1	0.71	0.24	0.30	0.46
AS	2	0.31	0.10	0.40	0.15
EB	2	0.98	0.33	0.23	0.37
GC	2	0.61	0.20	0.19	0.14
JC	2	0.68	0.23	0.18	0.21
KS	2	0.58	0.19	0.38	0.27
AS	3	1.08	0.36	0.31	0.80
EB	3	0.61	0.20	0.10	0.11
GC	3	0.68	0.23	0.17	0.38
JC	3	0.90	0.30	0.24	0.66
KS	3	0.78	0.26	0.18	0.37
AS	4	2.17	0.72	0.43	1.68
EB	4	1.05	0.35	0.20	0.50
GC	4	0.42	0.14	0.23	0.51
JC	4	1.81	0.60	0.33	1.22
KS	4	0.60	0.20	0.40	0.43

Table 4. Table of results of the orientation protocols for rater 2.

Orientation 1 (Modified Frankfort Horizontal) was found to have the least RSS for rater 1. Therefore, it was chosen as the method of orientation to use in Part 2 of the study, as rater 1 would be completing all of the orientations. In assessing inter-rater reliability, rater 2 was found to have an average increased RSS of 0.11 mm (Figures 23-24). This can be explained as rater 1 was more experienced with the landmark definitions, anatomy, and software. If all of the data from both raters are combined, as shown in Figure, Orientation 2 (Anatomage Default) has the lowest RSS. This is due to that fact that rater 2 was just as accurate as rater 1 using this orientation protocol.

As orientation 2 was found to be most reproducible and orientation 4 (NFZ) was least reproducible, a Student's t test was completed to compare the two. A statistically significant difference was found ($P<0.05$). However, orientations 1-3 showed no statistically significant differences; thus, it can be stated that all three have equivalent reproducibility. Although the differences were not found to be statistically significant, for rater1 the average RSS for each of the orientations was such that orientation 1 < 2 < 3. Error in degree of yaw for rater 1 was found such that orientation 1 < 2 < 3 < 4 (Figure 23). Error in degree of roll for rater 1 was found such that orientation 2 < 1 < 3 < 4. Error in degree of pitch for rater 1 was found such that orientation 2 < 1 < 3 < 4. The log transform of the RSS values was also completed to check for extreme outliers, but none were found.

Besides showing the overall RSS values for each orientation, Figure 25 also demonstrates that the error in yaw, roll, and pitch was less than 0.5°, except for the pitch in the NFZ orientation, which was 0.79°.

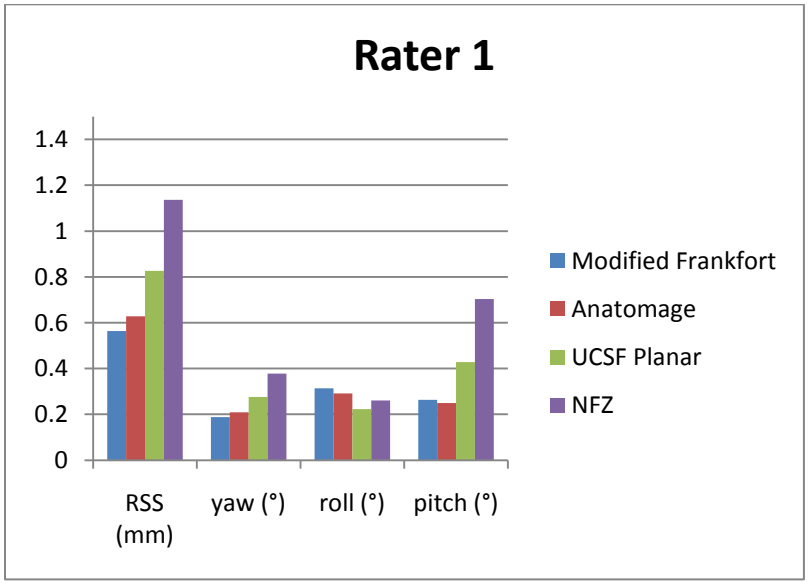

Figure 23. The mean error for each of the four orientation methods as completed by rater 1. The residual sum of squares (RSS) is reported in mm units, and the rotational errors in degrees.

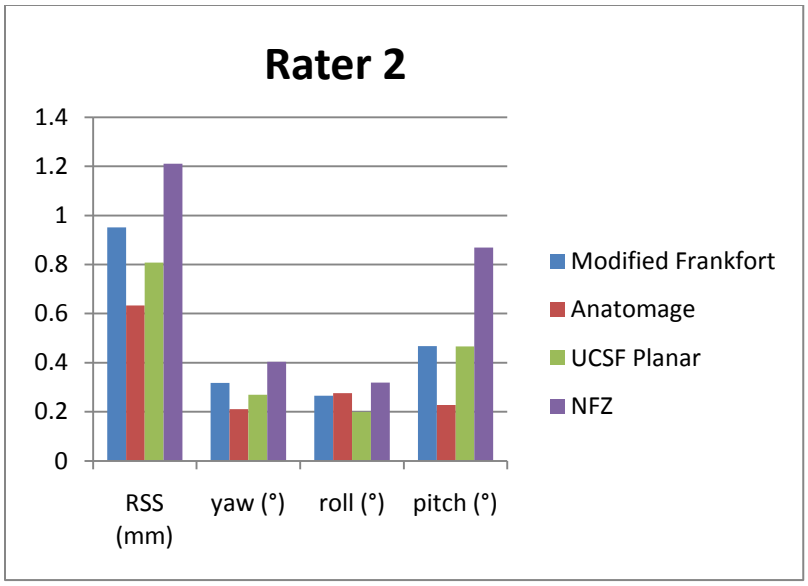

Figure 24. The mean error for each of the four orientation methods as completed by rater 1. The residual sum of squares (RSS) is reported in mm units, and the rotational errors in degrees.

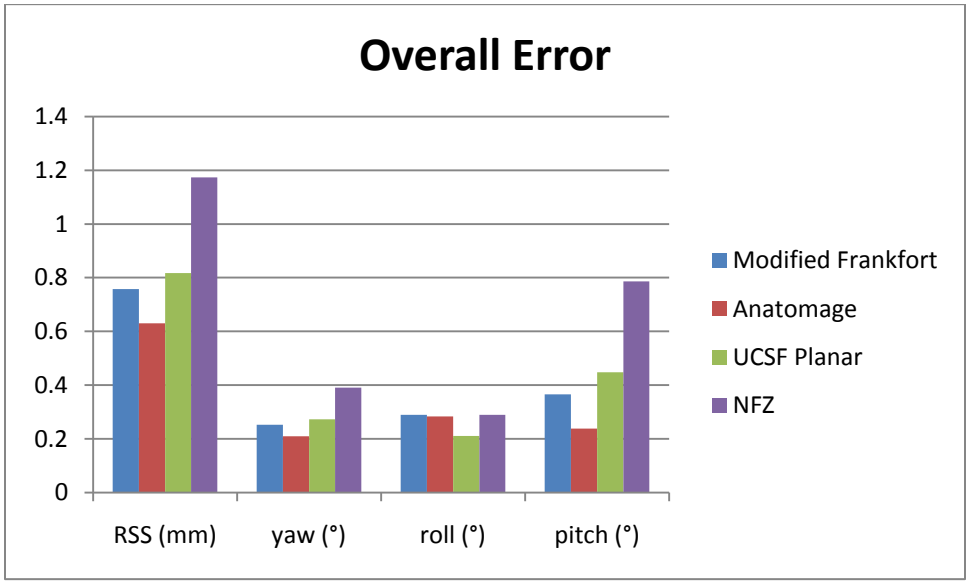

Figure 25. Overall error for each of the four orientation methods including data from both raters. The residual sum of squares (RSS) is reported in mm units, and the rotational errors in degrees. The RSS values show that the NFZ orientation had much higher error than the other three orientation methods.

Superimposition

Figure 26 shows the mean error between the superimposed volume to the original volumes over the three time points, with the mean and range displayed. As expected the landmarks farthest from the region of superimposition have the greatest mean error and the greatest outliers, including right and left gonion with vector errors of 0.19 mm and 0.16 mm, respectively. The greatest single linear error was found in the x-axis for gonion right at 0.36 mm, which can be considered subvoxel in size. The mean error vector for all of the landmarks was 0.12 mm with a standard deviation of 0.09 mm.

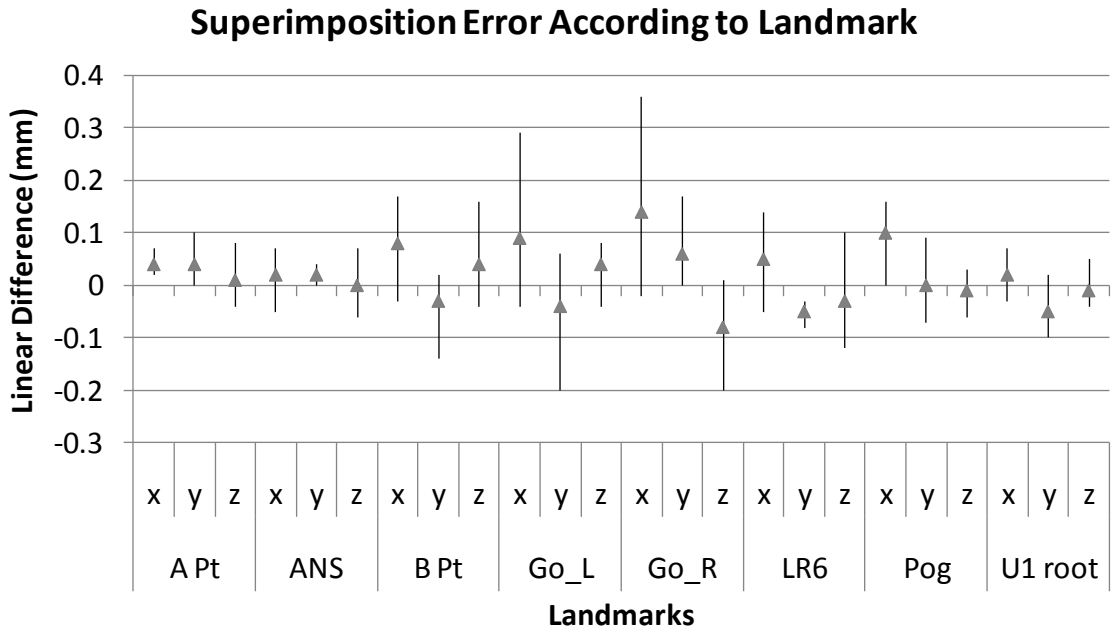

Figure 26. Figure demonstrating the mean error and the range of error in the x, y, and z axis between the superimposed volume to the original volume over the three time points.

For each of the three superimposition sessions, the mean centroid of the original scan landmark identification sessions were determined and compared to the mean centroid of the superimposed volume and the results are shown in Table 5. The mean error across the three

superimposition time points is the largest in the x-axis at 0.08 mm, with the error in the y- and z-axis being lower at 0.03 mm and 0.04 mm respectively.

Superimposition Time point	Horizontal (x) mm	Sagittal (y) mm	Vertical (z) mm	Vector
1	-0.02	-0.02	-0.02	0.03
2	0.08*	0.03*	-0.04	0.10
3	0.13*	-0.03*	0.05*	0.15
Mean	**0.08**	**0.03**	**0.04**	**0.09**

Table 5. Table showing the linear difference of the mean centroids of the original scans to the superimposed scans in the x, y, and z axis over the three superimposition time points. The vector of the mean error is also shown as is the mean linear error in each axis. *Statistically significant difference found between original and superimposed centroid location (P<0.05).

Student t-tests were completed to compare the centroids of the original and superimposed volume across the three landmark identification sessions for each of the three superimposition time points. Although the mean errors cannot be considered clinically significant, the centroid locations in the x and y axis for time point 2 were statistically significant (P<0.05) and for time point 3 across all three axes (P<0.05). This could be explained by either the superimposition error being statistically significantly large, or that the landmark identification for each of the scans had very low variability.

Part 2: Virtual 3D Orthognathic Treatment Simulation Accuracy

The linear results of the comparisons of the centroids of the prediction to the postsurgical outcomes for all nineteen surgeries and the degree of rotational differences are listed in Table 6. The actual difference between the presurgical scan and the postsurgical

outcome are listed in Table 7, along with the surgical notes. The signs of the differences in these tables represent direction. The differences were determined by subtracting the coordinates of the postsurgical outcome from the coordinates of the prediction. Therefore, a negative value represents a prediction that is right, forward, and down compared to the postsurgical outcome in the x, y, and z axis, respectively.

Patient	Horizontal (x) mm	Sagittal (y) mm	Vertical (z) mm	Vector difference mm	Yaw (°)	Roll (°)	Pitch (°)
Mn1	-0.49	-0.82	-0.51	1.08	-2.68	-0.95	-1.31
Mn2	-0.11	1.97	-1.79	2.66	-0.79	-0.72	-4.82
Mn3	-0.48	-0.52	-2.96	3.05	1.02	-1.75	2.18
Mn4	0.45	0.35	-3.41	3.46	-0.54	-0.41	-2.85
Mn5	-1.06	-0.10	-1.36	1.73	-0.69	0.20	2.26
Mn6	0.91	-0.86	0.07	1.25	3.37	1.23	2.26
Mn7	0.31	0.78	-1.31	1.55	0.63	0.21	-0.21
Mn8	-0.13	0.98	-2.16	2.38	-2.46	-0.40	0.95
Mn9	-0.12	0.07	-2.65	2.65	-0.58	-0.76	-0.06
Mn10	0.80	0.73	0.61	1.25	1.61	0.02	1.86
Mx1	0.08	1.70	1.61	2.35	-1.92	-0.26	-0.55
Mx2	-0.25	2.07	-0.12	2.09	-2.26	-1.11	-2.06
Mx3	-0.80	2.19	1.37	2.71	-0.60	0.64	2.00
Mx4	0.02	1.42	0.36	1.47	-1.25	0.10	-1.19
Mx5	0.72	2.18	-0.49	2.35	1.98	0.96	-6.22
Mx6	-0.50	0.73	0.49	1.01	0.63	0.55	0.88
Mx7	1.21	-1.85	-0.65	2.30	-0.05	-0.67	3.46
Mx8	1.08	0.69	0.55	1.39	-3.11	0.56	1.91
Mx9	0.14	0.31	0.26	0.43	-0.53	-0.56	0.22

Table 6. Comparison of prediction to postsurgical outcome showing linear, vector and angular differences.

Patient	Horizontal (x) mm	Sagittal (y) mm	Vertical (z) mm	Vector difference mm	Yaw (°)	Roll (°)	Pitch (°)	Surgical Notes
Mn1	1.92	4.10	1.76	4.86	5.26	1.12	5.59	7mm adv
Mn2	0.42	2.32	3.03	3.84	1.11	1.08	-0.86	7mm adv
Mn3	0.24	4.94	3.10	5.84	-1.31	1.60	-0.20	7mm adv
Mn4	-0.44	3.54	3.93	5.30	-0.74	-0.17	1.18	5mm adv
Mn5	-0.38	-3.70	-0.84	3.81	1.41	-0.08	-1.82	-4mm setback / 3mm rotation left
Mn6	0.74	-3.52	-1.48	3.89	-1.19	-0.94	3.48	?mm setback
Mn7	-0.37	3.06	2.74	4.12	-0.38	-0.16	0.91	6mm adv
Mn8	-1.69	0.55	1.30	2.20	-0.44	0.23	5.37	6mm adv
Mn9	0.47	5.78	1.73	6.05	0.95	0.63	-3.13	9mm adv / 1mm closure
Mn10	-0.42	4.92	1.75	5.24	-1.43	0.02	-2.71	10mm adv
Mx1	1.12	5.30	0.61	5.45	1.82	0.15	0.80	5mm adv
Mx2	-1.60	2.97	1.40	3.66	0.23	0.36	4.71	4mm adv/3mm rot left/ 1mm ant lengthen
Mx3	-0.71	6.72	-1.98	7.04	0.95	0.63	2.42	6mm adv
Mx4	1.16	3.66	1.52	4.13	2.49	0.08	-5.62	5mm adv / 3mm ant lengthen
Mx5	-1.17	1.61	4.83	5.22	-2.42	-1.26	3.73	6mm adv
Mx6	0.66	2.03	2.42	3.22	-0.52	-0.83	0.20	4mm adv / 4mm ant lengthen
Mx7	-0.76	1.02	-4.25	4.44	1.62	0.93	-1.63	5mm ant superior / 3mm post superior
Mx8	-2.35	5.70	0.36	6.18	1.79	-1.42	-3.74	5mm adv / 1mm rot right
Mx9	-1.29	4.68	0.57	4.89	-0.46	0.57	3.71	5mm adv

Table 7. Actual surgical change performed as measured from T0 to T1 (T0-T1) as compared to the surgical notes. Positive values represent right, anterior, and inferior movement of the respective jaw. For direction of rotations refer to Orientation 1 graphic in Figure 22

The differences between the landmarks of the superimpositions of the prediction and the surgical outcomes are shown in Figure 27, and the means and standard deviations are shown in Table 8. The means of the horizontal linear differences for both the maxillary and mandibular surgeries are less than 0.5 mm with standard deviations between 0.61-1.06 mm. The means for the sagittal differences for the mandibular surgeries are also less than 0.5 mm with standard deviations from 0.83 for the centrals up to 1.47 mm for the lower right first molar. The means for the vertical differences for maxillary surgeries was also less than 0.5mm with standard deviations between 0.82-1.22 mm. The greatest variability was found in the vertical linear differences in the mandibular surgeries (SD: 1.67, 1.09, and 1.52 mm for the three landmarks) and in the sagittal differences in the maxillary surgeries (SD: 1.61, 1.80 and 1.35).

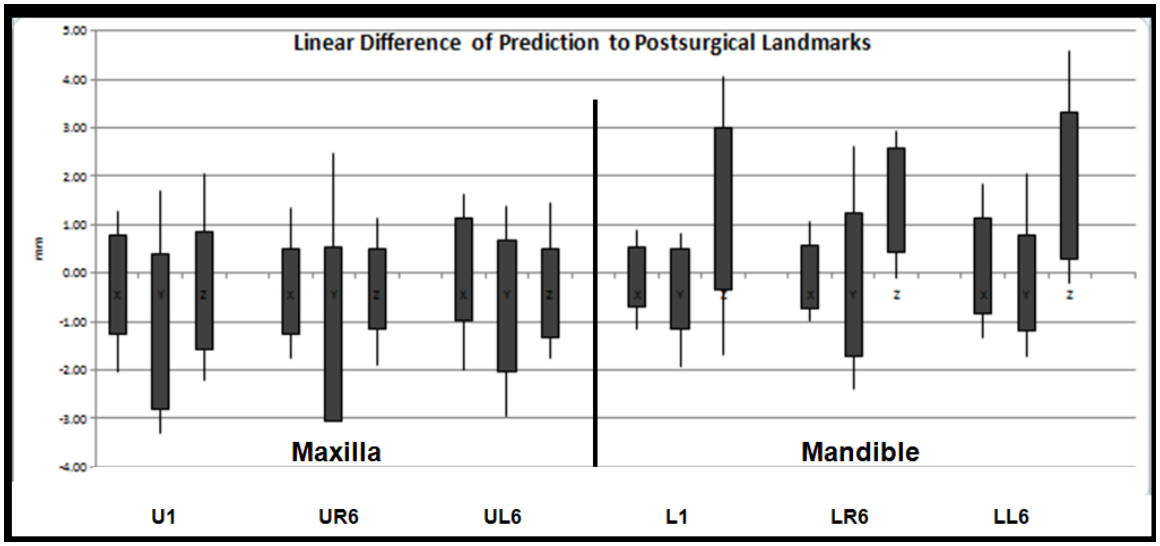

Figure 27. Linear difference of prediction to postsurgical landmarks. Box plot shows mean +/- SD, with lines representing the max and min outliers of all 19 surgical predictions.

Landmark	Horizontal (x) mm			Sagittal (y) mm			Vertical (z) mm		
	Mean	Abs Mean	SD	Mean	Abs Mean	SD	Mean	Abs Mean	SD
U1	-0.25	0.78	1.02	-1.21	1.62	1.61	-0.38	0.98	1.22
UR6	-0.39	0.77	0.89	-1.27	1.81	1.80	-0.34	0.66	0.82
UL6	0.07	0.80	1.06	-0.68	1.24	1.35	-0.41	0.80	0.92
L1	-0.08	0.46	0.61	-0.32	0.65	0.83	1.34	1.83	1.67
LR6	-0.08	0.55	0.65	-0.25	1.09	1.47	1.51	1.54	1.09
LL6	0.13	0.76	0.98	-0.21	0.69	0.99	1.80	1.86	1.52

Table 8. Linear difference of prediction to postsurgical landmarks with mean and magnitude of the mean differences (mean of the absolute value of the error) for each axis along with the standard deviations listed.

The signs of the differences in Figure 27 also represent direction. The negative mean values of the maxillary landmarks in the sagittal demonstrate that the postsurgical outcome was

consistently less anterior than the prediction shows. Also, the positive mean values of the mandibular landmarks in the vertical dimension demonstrate that the mandibular surgical outcome was consistently further downward than the prediction. This can be explained as splints were present in seven of the ten mandibular surgeries at time of postsurgical CBCT. The three surgeries without splints (Mn1, 6, and 10) showed a statistically significant smaller error in the vertical dimension ($P < 0.01$) than those with a splint, with mean linear vertical difference of 0.40 mm compared to 2.23 mm for the seven mandibular surgeries with the splint in place.

Student t-tests were completed to compare for differences between the right and left sides. The right and left landmarks for the surgeries did not show any statistical significant differences.

The linear differences between the centroids of the prediction and the postsurgical outcomes of the mandibular and maxillary surgeries are graphed in Figure 28 with the direction of the differences shown.

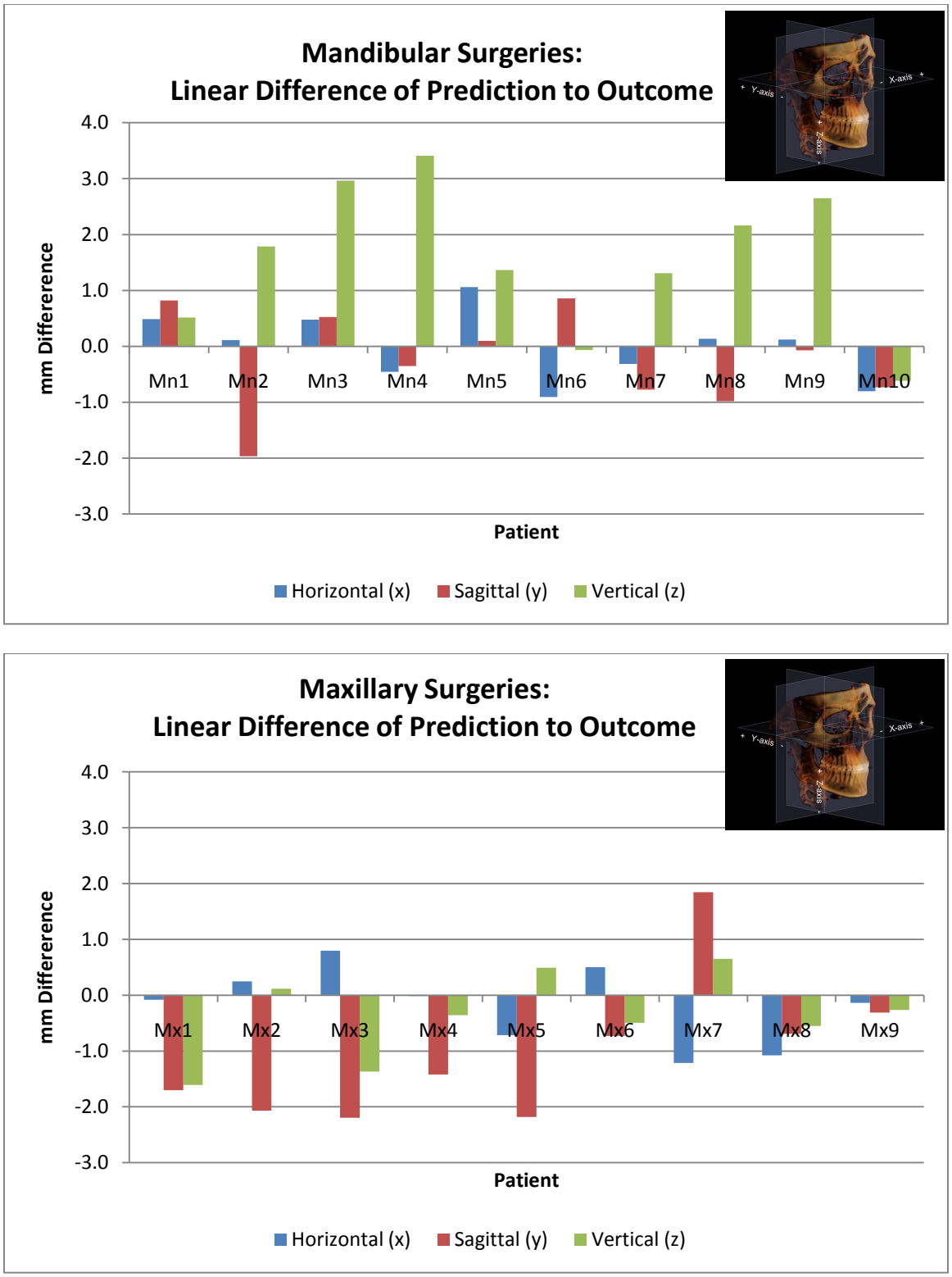

Figure 28. Linear differences of prediction and postsurgical outcome according to axis with sign representing direction of difference. Top) Mandibular Surgeries. Bottom) Maxillary Surgeries

The relative magnitudes of the differences are graphed in Figure 29 according to axis. The mean and standard deviations of the centroid differences for the maxillary and mandibular surgeries are listed in Table 9. The mean linear differences for all the surgeries were found to be 0.51 mm horizontally, 1.07 mm in the AP, and 1.20 mm vertically.

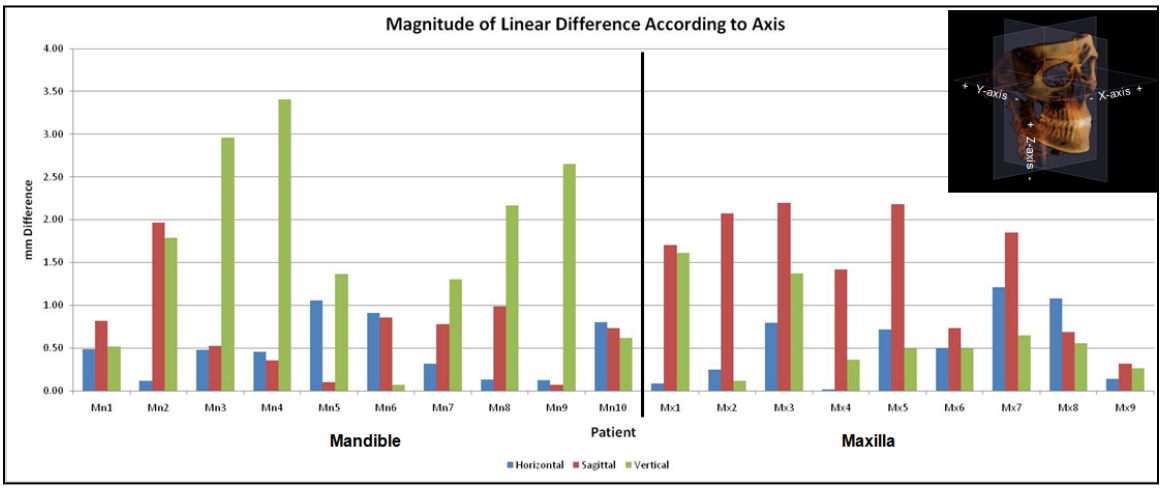

Figure 29. Absolute value of the linear differences between prediction and postsurgical outcome according to axis demonstrating relative magnitude of the differences.

Surgery	Horizontal (x) mm		Sagittal (y) mm		Vertical (z) mm		Vector mm	
	Mean	SD	Mean	SD	Mean	SD	Mean	SD
Maxilla	0.53	0.69	1.46	1.29	0.66	0.76	1.79	0.75
Mandible	0.49	0.61	0.72	0.89	1.68	1.31	2.11	0.84
Max & Mand	0.51	0.64	1.07	1.14	1.20	1.45	1.96	0.79

Table 9. Linear differences between prediction and postsurgical outcome showing maxillary surgeries, mandibular surgeries, and the overall results for all surgeries. Means of the magnitude of the differences are reported.

The angular differences of the prediction and the postsurgical outcomes of the mandibular and maxillary surgeries are graphed in Figure 30.

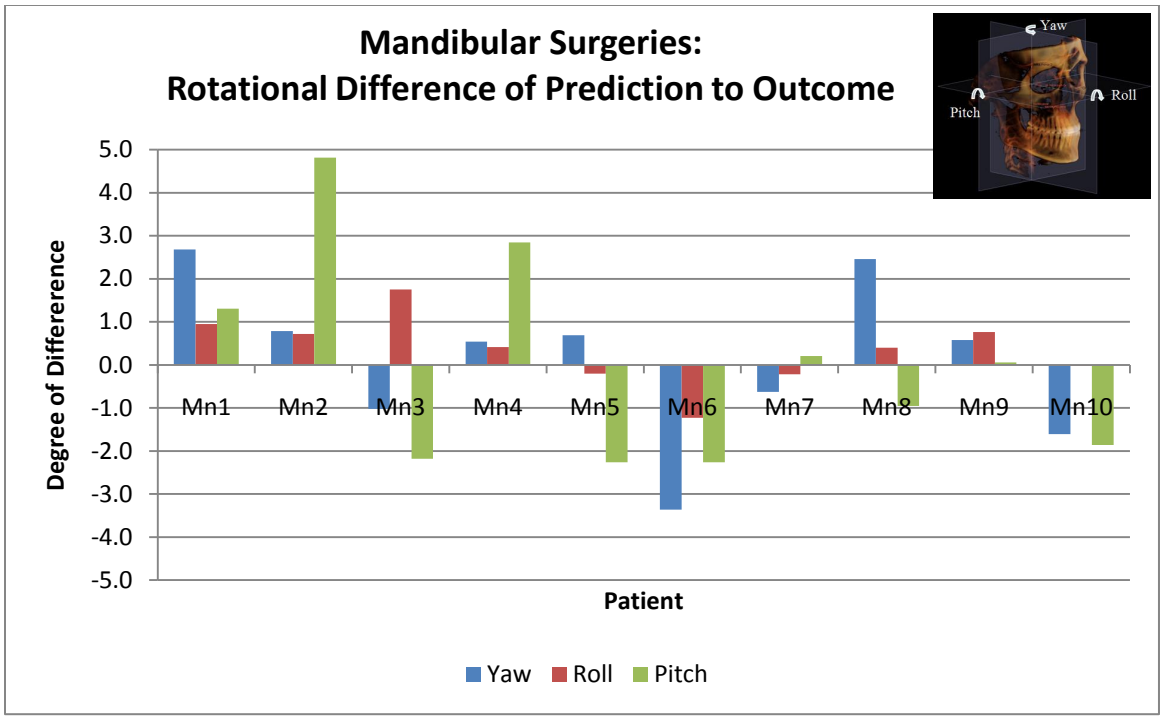

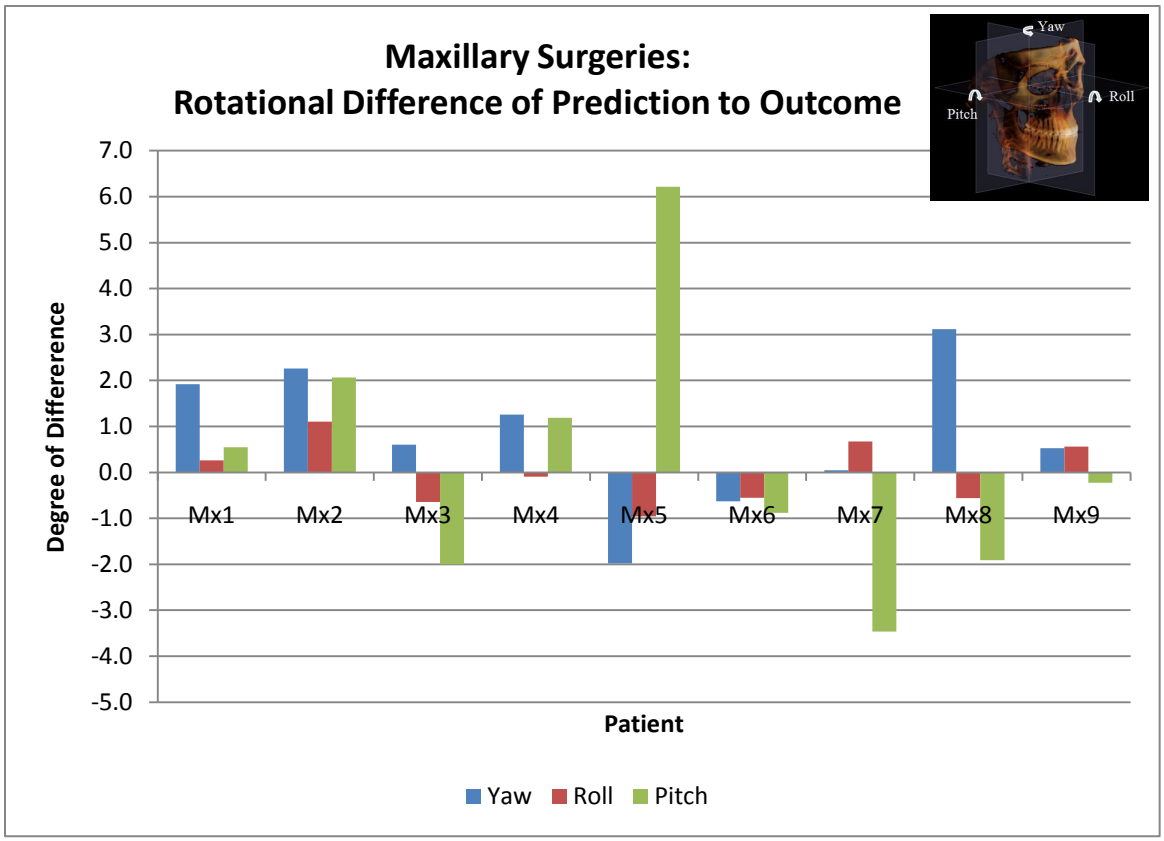

Figure 30. Angular differences of prediction and postsurgical outcome according to axis with sign representing direction of rotation. Note: arrows in graphic represent positive direction. Top) Mandibular Surgeries. Bottom) Maxillary Surgeries

The relative magnitudes of the angular differences are graphed in Figure 31 according to axis. The mean and standard deviations of the angular differences for the maxillary and mandibular surgeries are listed in Table 10. The mean rotational differences were found to be 1.41° around the z axis (yaw), 0.64° around the y axis (roll), and 1.96° around the x axis (pitch).

The error in maxillary pitch was higher than expected due to an outlier, Mx5 surgery, in which during surgery the anterior maxilla was disimpacted more than was recorded in the surgical notes. If the mean of the maxillary pitch was adjusted for this outlier, the maxillary pitch mean would be 1.54° (SD 1.04) instead of 2.06° (SD 2.84).

Predictions of both maxillary and mandibular surgeries are most accurate in predicting rotations around the y-axis (roll) and least accurate in predicting the rotation around the x-axis (pitch) and around the z-axis (yaw).

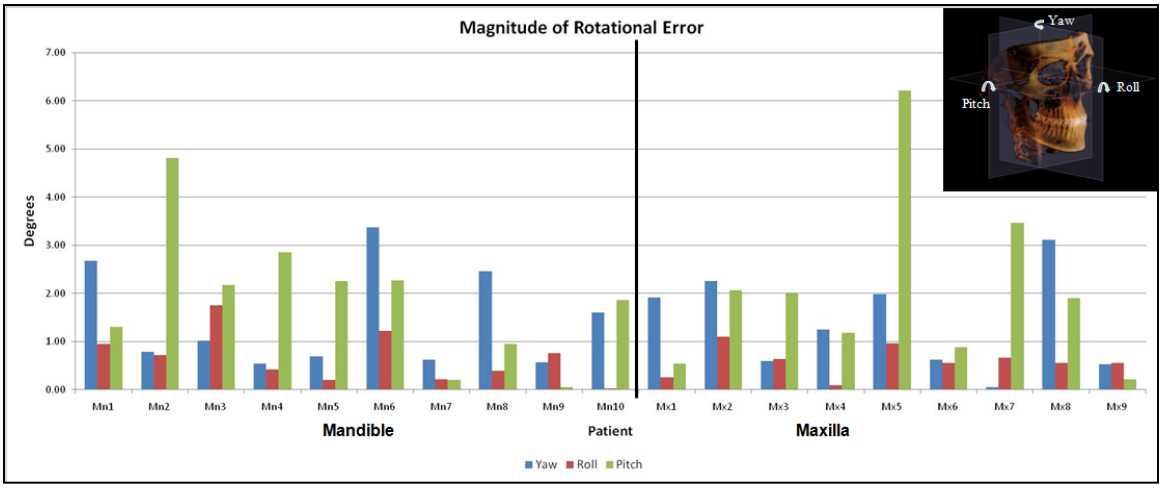

Figure 31. Absolute value of the angular differences between prediction and postsurgical outcome according to axis demonstrating the relative magnitude of the differences.

Surgery	Roll		Pitch		Yaw	
	Mean	*SD*	*Mean*	*SD*	*Mean*	*SD*
Maxilla (°)	0.60	0.71	2.06	2.85	1.37	1.56
Mandible (°)	0.66	0.81	1.88	2.41	1.44	1.83
Max & Mand (°)	0.64	0.76	1.96	2.55	1.41	1.70

Table 10. Angular differences between prediction and postsurgical outcome. Means of the magnitude of the differences are reported, as well as the standard deviations.

Maxillary surgeries and mandibular surgeries were compared using Student's t test, with results listed in Table 11. Predictions in the sagittal and vertical dimension were found to be statistically significantly different ($P<0.05$) for the mandibular surgeries compared to the maxillary surgeries. Horizontal translation and none of the rotations were found to be statistically significant when comparing maxillary to mandibular surgical predictions. Predictions of both maxillary and mandibular surgeries have the least error in predicting the final horizontal position and the amount of rotation around the y-axis (roll).

	Maxillary Mean	Mandibular Mean	Maxillary SD	Mandibular SD	t Stat	P Value
Horizontal (mm)	0.53	0.49	0.69	0.61	-0.2516	0.4022
Sagittal (mm)	1.46	0.72	1.29	0.89	-2.5713	0.0099*
Vertical (mm)	0.66	1.68	0.76	1.31	2.5382	0.0106*
Vector (mm)	1.79	2.11	0.75	0.84	0.8639	0.1998
Yaw (°)	1.37	1.44	1.56	1.83	0.1383	0.4458
Roll (°)	0.60	0.66	0.71	0.81	0.3114	0.3796
Pitch (°)	2.06	1.88	2.85	2.41	-0.2409	0.4063

Table 11. Comparison of maxillary and mandibular surgeries. *Sagittal and vertical linear differences were found to be statistically significant (P<0.5).

Discussion

This study shows that one can effectively use a commercial software application that is readily available to the clinical and academic fields to plan and predict the effects of orthognathic surgery. The potential of planning the entire orthognathic surgery on one software has far-reaching implications as it allows the clinician to evaluate the surgery from any perspective, any plane, and from a volumetric view from any direction. More importantly, further development of such software provides a method for the clinician to fabricate dental splints which could be used in the surgical suite to complement a computer monitor displaying a volumetric view of the before and predicted surgical changes.

However, to complete such studies using superimposition, it is evident from this work that the capability to orient the head of each subject in a systematic and reproducible manner is vital before the software can be applied. In addition, the orientation has to have a noise level in its application below that of the surgical changes planned. Evaluating an object in three-

dimensional space, and how it will be repositioned surgically, requires determining six degrees of freedom that are expressed in three planes as well as around three axes. Such evaluations are highly accurate with cone beam computed tomography-generated data in DICOM format due to the accuracy of the three dimensional coordinate system and of the actual volume being evaluated which, in this case, refers to the craniofacial region.

The value of this study is two-fold. It first provides a method to determine the actual surgical outcome in three dimensions. Secondly, it compares that surgical outcome to a prediction of what the surgeon wanted to achieve in that patient. While this works well with a surface-rendered hard tissue like the cranioskeleton and mandible, it has difficulty in predicting the effect on soft tissue overlying the bone as with the lips and chin. In addition, evaluating the occlusion depends on the resolution and quality of the CBCT scan as well as whether the teeth are apart during the CBCT scan, which creates an additional factor that can affect the vertical changes predicted.

CBCT provides a major advancement in orthodontics and orthognathic surgery as it now provides a method to assess how the form changes with the surgery and improves on previous attempts to evaluate surgery two-dimensionally which emphasized vertical changes and rotational changes around the condyle before and after orthognathic surgery (Ellis, 2011). Studies by several investigators have emphasized that the form needs to be evaluated using programs like thin plate spline analysis, but have had to project the changes based on changes in landmarks (Bookstein 1996).

CBCT provides accurate assessment of the real shape and its change in position but requires several restrictions to be functional in the average clinician or academic setting. Ideally, three-dimensional forms should be real volumes and not surface rendered volumes, and

comparing two or three different volumes with superimpositions should be done with the entire volume through complex mathematical processes. Unfortunately, computer power available to most investigators is restricted so that only a small region of the craniofacial area, like a portion of the cranial base, can be used to superimpose two craniofacial regions through a method like the procrustes analysis (Cevidanes 2006). The alternative is to define landmarks in the cranial base for superimpositions, (Lagravere and Major 2010) and then use landmarks on regions of the maxilla and mandible to follow how the entire structure moves. The identity and location of the landmarks then is the standard to work with the three-dimensional structure, and, ideally, the location of each landmark should have an error less than what would be expected with the orthognathic surgery.

Orienting the Head

The Modified Frankfort Horizontal orientation method was determined in Part 1 to be the most reproducible for rater 1 based on the residual sum of squares (RSS). However, when including both raters, the Anatomage Default orientation method had the lowest RSS. Statistical analysis did not show any significant difference between the two methods, so they could be used interchangeably. However, an experienced user can expect lower error with the Modified Frankfort Horizontal protocol. Given that both raters had similar error with the Anatomage Default orientation, this orientation is less reliant on the experience of the user. Therefore, even a novice user can expect high orientation reproducibility with the Anatomage default. In addition, further statistical analysis could be undertaken to determine the variation of each plane in terms of rotation and translation for each of the four methods, and possibly determine a new orientation method combining the best of each of the four examined in this study.

Measurements in Three Dimensions

Some of the quantitative results in this study could be compared with previous 2D studies (*i.e.,* results when the x or y axis is set to zero). However, when working in three dimensions, an evaluation of the accuracy can be undertaken in all three directions of translation as well as rotation around each axis. Therefore, a comparison with previous 3D studies would be most valuable.

Xia *et al.,* found the median differences between planned and actual postoperative outcomes to be 0.9 mm and 1.7 degrees (Xia, Gateno et al. 2007). In their analysis of five cases, the results were reported in terms of the largest linear distance in only one dimension, not as a vector. Also, the means reported by Xia *et al.,* did not appear to be the means of the magnitude of the differences, but rather the mean of the differences including the signs, which would lead to means closer to zero. The mean magnitude error would have been a better representation of the error observed between prediction and outcome. This study was also limited due to its very small sample size of five patients. The greatest mean magnitude error for all nineteen surgeries in any one direction was found to be 1.20 mm in our study and 1.96 degrees, which are comparable to previous findings.

Maxillary Predictions

As stated in the Results section, maxillary predictions were found to be least accurate in determining final sagittal position. This could be explained if the presurgical scan had a CR-CO shift. A patient postured forward in the presurgical scan would lead to a virtual surgery with an over advanced maxilla. Or, the results could suggest that the maxilla was under advanced. Previous studies based on lateral headfilms had similar finding when comparing predictions to postsurgical outcomes (Sharifi, Jones et al. 2008). Sharifi *et al.,* found that the maxilla showed a

tendency for under-advancement compared with the predicted movement in about 33% of the cases in both groups.

Planning Virtual Surgeries

Surgical notes were used in order to conduct the virtual surgeries. The notes did not always represent what actually transpired in surgery. Although surgical notes alone would not provide the level of accuracy that we would like to evaluate in this study, when used in conjunction with knowledge of the treatment goals, the surgical notes can be a good approximation for guiding the virtual surgery. As this retrospective study was limited to the use of surgical notes, the surgical samples in this study were limited to single jaw surgery patients. This limits the variability that could be expected from using surgical notes alone to perform and evaluate virtual 2-jaw surgeries. It can be argued that predictions based on surgery notes are themselves not an accurate representation of the actual surgical outcomes (Tucker, Cevidanes et al.). However, by limiting our samples to single jaw surgeries, we were able to limit the variability enough so that we could evaluate the prediction process as a whole and draw conclusions on the prediction accuracy as well as evaluate the software.

This study was limited to single jaw surgeries, but the clear benefits of virtual surgery seem to lie in 2-jaw surgeries. Bi-maxillary surgery has been shown to be more challenging to predict than single jaw surgery (Jacobson and Sarver 2002). Although Tucker *et al.,* (Tucker, Cevidanes et al.) indicate that their research showed no difference between "predictions" of 1- vs 2-jaw surgery patients, this is to be expected given the methods used where the virtual models were simply overlaid on the postsurgical models. This methodology confirmed the accuracy of the software used, but not the actual prediction process and, therefore, a difference in 1- vs 2-jaw surgeries would not be expected. In the future, a prospective study using the

techniques described in this study to evaluate 1- and 2-jaw surgeries would be of great value. This would preclude the issue of performing the "predictions" based on surgical notes, and 2-jaw surgeries could be evaluated, which seem to be the cases that would mostly benefit from virtual surgery planning.

Accuracy of Simulation

This study demonstrated that InvivoDental can accurately simulate the actual outcomes of single jaw surgery to a similar level of accuracy as has been shown in the past for 2 dimensional predictions (Donatsky, Hillerup et al. 1992; Donatsky, Bjorn-Jorgensen et al. 1997). Addition of more detailed dental anatomy from laser scans to the CBCT-based virtual models could improve the accuracy of these simulations and allow for splint fabrication. Splint fabrication in conjunction with the use of an intraoperative navigation system could assist the surgeon in translating the predictions to the actual surgery.

The resolution and accuracy of a CBCT scan is not high enough to shape exact teeth (Santler, Karcher et al. 1998), and artifacts from fillings and crowns create additional inaccuracies (Nkenke, Zachow et al. 2004). It can be expected that the accuracy of the virtual simulations reported in this study would be improved by including a registration of detailed dental anatomy from imaging of dental casts, as has been advocated by many other investigators (Xia, Ip et al. 2000; Gateno, Xia et al. 2003; Uechi, Okayama et al. 2006; Swennen, Mollemans et al. 2009; Swennen, Mommaerts et al. 2009). However, even this registration process has been shown to have some error associated with it. Uechi *et al.,* (Uechi, Okayama et al. 2006) reported registration errors for their simulation system of less than 1 mm with the root mean square error being less than 0.4 mm in two patients. Using a double CBCT scan procedure for capturing the detailed dental surfaces, Swennen *et al.,* reported mean

registration error for automatic point-based rigid registration of 0.18 ± 0.10 mm (range 0.13–0.26 mm) (Swennen, Mommaerts et al. 2009). Nkeneke *et al.,* reported statistically significant differences in registration accuracy of CT scans with metal fillings compared to those without such fillings (Nkenke, Zachow et al. 2004).

Segmentation and Virtual Models

The virtual models in this study were created through the process of segmentation of the bone and tooth surfaces by applying a threshold on the volume of the radiographic densities. In cases where the opposing dentition was in contact, manual segmentation was used to separate the teeth, which is a user-dependent procedure that is very time-consuming and must be associated with some degree of error. To account for any error in this segmentation protocol, a landmark was identified on the original presurgical scan and on the virtual model. The difference between these landmarks was calculated and then applied to the prediction virtual model to account for any segmentation errors. The average segmentation adjustment in any one direction was 0.2 mm. The greatest segmentation error was in the vertical dimension for the landmarks on the 6s due to the manual segmentation procedure and the thresholding protocol which tended to overestimate the size of the dental crowns. These errors could have been avoided or minimized through the registration of a detailed dental anatomy scan to the CBCT as described above.

Limitations of Virtual Simulation

Although 3D virtual simulation has many benefits over the conventional technique as described previously, one advantage of the conventional model surgery is that the postsurgical occlusal relationship is manually determined by haptic sensation. In a virtual environment, the

user is limited to the visual sense and, thus, determining the occlusion can be a time-consuming process. There have been attempts to address this problem in the software with collision detection systems (Troulis, Everett et al. 2002). Collision detection systems have disadvantages in that complex dental anatomy can cause inaccuracies in fitting; although there is ongoing work on increasing the accuracy of these algorithms (Hu, Langlotz et al. 2001). Uechi *et al.,* (Uechi, Okayama et al. 2006) designed a simulation workflow that avoids this issue by occluding the preoperative dental casts prior to imaging them, in order to bypass the need for virtual determination of occlusion. Our study incorporated only visual detection of the occlusion. As the algorithms improve for collision detection, future studies should attempt to incorporate them into the software to determine the occlusion. By requiring dental casts to determine the desired occlusal relationship such as proposed by Uechi, some of the advantages of virtual surgery would be lost, such as material and time savings (Xia, Phillips et al. 2006). In addition, multiple piece surgical procedures would require sectioning of the casts and an attempt to register these segmented models to the virtual models would be challenging.

Virtual surgery has been shown to be at least as accurate as conventional prediction techniques, yet offers many benefits including reduced patient and surgeon time as well as lower material costs (Xia, Phillips et al. 2006). As the price of the software and 3D printers drop, the material costs savings will continue to improve. Preoperative virtual surgery allows the surgeon to better understand the three-dimensional impact of the planned surgery as well as better predict possible surgical complications. It also allows for complex cases to potentially be performed in a single procedure instead of staged surgeries (Gateno, Xia et al. 2007).

Now that virtual surgical simulations have been validated in this retrospective study, more research should be conducted to determine the accuracy of this technique in a prospective study. This study was limited by the use of surgical notes as a guide for the

simulation. Surgical notes may not accurately represent the actual surgery performed in the operating room. In a prospective study, the surgeon can be involved in the simulation before surgery and actually plan the surgery using the software. This would create a true prediction that could be used to create a stereolithographic surgical splint to be used in the surgery. Prior to using these splints in a patient surgery, a comparative study should be performed of surgical splints fabricated from stereolithographic models produced from virtual surgeries vs. traditional splints from model surgery. If the results are promising, then the prospective study to evaluate the use of computer generated splints in surgery reduces variability of surgical outcomes, and increases predictability of surgery can be undertaken.

CONCLUSIONS

Overall, the mean error was found to be < 2mm linearly and < 2° angularly, which is comparable to the findings in 2D studies. Specifically, mean linear differences were found to be 0.51 mm horizontally, 1.07 mm anteroposteriorly, and 1.20 mm vertically. Mean rotational differences were found to be 1.41° around the z axis (yaw), 0.64° around the y axis (roll), and 1.96° around the x axis (pitch). The maxillary surgery error for the linear measurements ranked for the linear with: Horizontal < Vertical < Sagittal, and for the angular: Roll < Yaw < Pitch. The mandibular surgery error for the linear was: Horizontal < Sagittal < Vertical, and for the angular: Roll < Yaw < Pitch.

Virtual simulation of orthognathic surgery using InVivoDental software closely approximates the final outcome. This protocol can be used as a tool for surgical planning and splint fabrication.

REFERENCES

Baumrind, S. and R. C. Frantz (1971). "The reliability of head film measurements. 1. Landmark identification." Am J Orthod **60**(2): 111-27.

Bell, R. B. (2011). "Computer planning and intraoperative navigation in orthognathic surgery." J Oral Maxillofac Surg **69**(3): 592-605.

Bjork, A. and V. Skieller (1983). "Normal and abnormal growth of the mandible. A synthesis of longitudinal cephalometric implant studies over a period of 25 years." Eur J Orthod **5**(1): 1-46.

Bookstein, F. L. (1996). "Biometrics, biomathematics and the morphometric synthesis." Bull Math Biol **58**(2): 313-65.

Carvalho Fde, A., L. H. Cevidanes, et al. "Three-dimensional assessment of mandibular advancement 1 year after surgery." Am J Orthod Dentofacial Orthop **137**(4 Suppl): S53 e1-12; discussion S53-5.

Cevidanes, L. H., L. J. Bailey, et al. (2005). "Superimposition of 3D cone-beam CT models of orthognathic surgery patients." Dentomaxillofac Radiol **34**(6): 369-75.

Cevidanes, L. H., G. Heymann, et al. (2009). "Superimposition of 3-dimensional cone-beam computed tomography models of growing patients." Am J Orthod Dentofacial Orthop **136**(1): 94-9.

Cevidanes, L. H., M. A. Styner, et al. (2006). "Image analysis and superimposition of 3-dimensional cone-beam computed tomography models." Am J Orthod Dentofacial Orthop **129**(5): 611-8.

Chapuis, J., A. Schramm, et al. (2007). "A new system for computer-aided preoperative planning and intraoperative navigation during corrective jaw surgery." IEEE Trans Inf Technol Biomed **11**(3): 274-87.

Chew, M. T., C. H. Koh, et al. (2008). "Subjective evaluation of the accuracy of video imaging prediction following orthognathic surgery in Chinese patients." J Oral Maxillofac Surg **66**(2): 291-6.

Choi, J. Y., K. G. Song, et al. (2009). "Virtual model surgery and wafer fabrication for orthognathic surgery." Int J Oral Maxillofac Surg **38**(12): 1306-10.

de Oliveira, A. E., L. H. Cevidanes, et al. (2009). "Observer reliability of three-dimensional cephalometric landmark identification on cone-beam computerized tomography." Oral Surg Oral Med Oral Pathol Oral Radiol Endod **107**(2): 256-65.

Dean, D., M. G. Hans, et al. (2000). "Three-dimensional Bolton-Brush Growth Study landmark data: ontogeny and sexual dimorphism of the Bolton standards cohort." Cleft Palate Craniofac J **37**(2): 145-56.

Donatsky, O., J. Bjorn-Jorgensen, et al. (1997). "Computerized cephalometric evaluation of orthognathic surgical precision and stability in relation to maxillary superior repositioning combined with mandibular advancement or setback." J Oral Maxillofac Surg **55**(10): 1071-9; discussion 1079-80.

Donatsky, O., S. Hillerup, et al. (1992). "Computerized cephalometric orthognathic surgical simulation, prediction and postoperative evaluation of precision." Int J Oral Maxillofac Surg **21**(4): 199-203.

Ellis, E., 3rd (1990). "Accuracy of model surgery: evaluation of an old technique and introduction of a new one." J Oral Maxillofac Surg **48**(11): 1161-7.

Gateno, J., J. Xia, et al. (2003). "A new technique for the creation of a computerized composite skull model." J Oral Maxillofac Surg **61**(2): 222-7.

Gateno, J., J. J. Xia, et al. (2007). "Clinical feasibility of computer-aided surgical simulation (CASS) in the treatment of complex cranio-maxillofacial deformities." J Oral Maxillofac Surg **65**(4): 728-34.

Gliddon, M. J., J. J. Xia, et al. (2006). "The accuracy of cephalometric tracing superimposition." J Oral Maxillofac Surg **64**(2): 194-202.

Hatcher, D. C. and C. L. Aboudara (2004). "Diagnosis goes digital." Am J Orthod Dentofacial Orthop **125**(4): 512-5.

Haynes, S. and M. N. Chau (1993). "Inter- and intra-observer identification of landmarks used in the Delaire analysis." Eur J Orthod **15**(1): 79-84.

Hu, Q., U. Langlotz, et al. (2001). "A fast impingement detection algorithm for computer-aided orthopedic surgery." Comput Aided Surg **6**(2): 104-10.

Jacobson, R. and D. M. Sarver (2002). "The predictability of maxillary repositioning in LeFort I orthognathic surgery." Am J Orthod Dentofacial Orthop **122**(2): 142-54.

Kaipatur, N., Y. Al-Thomali, et al. (2009). "Accuracy of computer programs in predicting orthognathic surgery hard tissue response." J Oral Maxillofac Surg **67**(8): 1628-39.

Kaipatur, N. R. and C. Flores-Mir (2009). "Accuracy of computer programs in predicting orthognathic surgery soft tissue response." J Oral Maxillofac Surg **67**(4): 751-9.

Kiyak, H. A. and R. Bell (1991). Psychosocial considerations in surgery and orthodontics. Surgical Orthodontic Treatment. W. Proffit and R. P. White, Jr. St Louis, Mosby**:** 71-95.

Lagravere, M. O., C. Low, et al. "Intraexaminer and interexaminer reliabilities of landmark identification on digitized lateral cephalograms and formatted 3-dimensional cone-beam computerized tomography images." Am J Orthod Dentofacial Orthop **137**(5): 598-604.

Mah, J. and D. Hatcher (2004). "Three-dimensional craniofacial imaging." Am J Orthod Dentofacial Orthop **126**(3): 308-9.

Mah, J. K., J. C. Huang, et al. "Practical applications of cone-beam computed tomography in orthodontics." J Am Dent Assoc **141 Suppl 3**: 7S-13S.

Maki, K., N. Inou, et al. (2003). "Computer-assisted simulations in orthodontic diagnosis and the application of a new cone beam X-ray computed tomography." Orthod Craniofac Res **6 Suppl 1**: 95-101; discussion 179-82.

Mankad, B., G. J. Cisneros, et al. (1999). "Prediction accuracy of soft tissue profile in orthognathic surgery." Int J Adult Orthodon Orthognath Surg **14**(1): 19-26.

Meehan, M., M. Teschner, et al. (2003). "Three-dimensional simulation and prediction of craniofacial surgery." Orthod Craniofac Res **6 Suppl 1**: 102-7.

Melsen, B. (1974). "The cranial base." Acta Odontol Scand **32**(Suppl 62): 86-101.

Miller, A. J., K. Maki, et al. (2004). "New diagnostic tools in orthodontics." Am J Orthod Dentofacial Orthop **126**(4): 395-6.

Nkenke, E., S. Zachow, et al. (2004). "Fusion of computed tomography data and optical 3D images of the dentition for streak artefact correction in the simulation of orthognathic surgery." Dentomaxillofac Radiol **33**(4): 226-32.

Olszewski, R. and H. Reychler (2004). "[Limitations of orthognathic model surgery: theoretical and practical implications]." Rev Stomatol Chir Maxillofac **105**(3): 165-9.

Padwa, B. L., M. O. Kaiser, et al. (1997). "Occlusal cant in the frontal plane as a reflection of facial asymmetry." J Oral Maxillofac Surg **55**(8): 811-6; discussion 817.

Pektas, Z. O., B. H. Kircelli, et al. (2007). "The accuracy of computer-assisted surgical planning in soft tissue prediction following orthognathic surgery." Int J Med Robot **3**: 64-71.

Perillo, M., R. Beideman, et al. (2000). "Effect of landmark identification on cephalometric measurements: guidelines for cephalometric analyses." Clin Orthod Res **3**(1): 29-36.

Phillips, C., B. J. Hill, et al. (1995). "The influence of video imaging on patients' perceptions and expectations." Angle Orthod **65**(4): 263-70.

Proffit, W., R. P. White, Jr., et al. (2002). Contemporary Treatment of Dentofacial Deformity. St Louis, Mosby.

Proffit, W. R., T. A. Turvey, et al. (2007). "The hierarchy of stability and predictability in orthognathic surgery with rigid fixation: an update and extension." Head Face Med **3**: 21.

Richardson, A. (1966). "An investigation into the reproducibility of some points, planes, and lines used in cephalometric analysis." Am J Orthod **52**(9): 637-51.

Santler, G., H. Karcher, et al. (1998). "Indications and limitations of three-dimensional models in cranio-maxillofacial surgery." J Craniomaxillofac Surg **26**(1): 11-6.

Sarver, D. M., M. W. Johnston, et al. (1988). "Video imaging for planning and counseling in orthognathic surgery." J Oral Maxillofac Surg **46**(11): 939-45.

Schlicher, W., I. Nielsen, et al. "Consistency and precision of landmark identification in three-dimensional cone beam computed tomography scans." Eur J Orthod.

Semaan, S. and M. S. Goonewardene (2005). "Accuracy of a LeFort I maxillary osteotomy." Angle Orthod **75**(6): 964-73.

Sharifi, A., R. Jones, et al. (2008). "How accurate is model planning for orthognathic surgery?" Int J Oral Maxillofac Surg **37**(12): 1089-93.

Smith, J. D., P. M. Thomas, et al. (2004). "A comparison of current prediction imaging programs." Am J Orthod Dentofacial Orthop **125**(5): 527-36.

Sohmura, T., H. Hojo, et al. (2004). "Prototype of simulation of orthognathic surgery using a virtual reality haptic device." Int J Oral Maxillofac Surg **33**(8): 740-50.

Solow, B. (1966). "The Pattern of Craniofacial Associations." Acta Odontol Scand **24 (Supplementum 46)**: 26.

Stabrun, A. E. and K. Danielsen (1982). "Precision in cephalometric landmark identification." Eur J Orthod **4**(3): 185-96.

Swennen, G. R., W. Mollemans, et al. (2009). "Three-dimensional treatment planning of orthognathic surgery in the era of virtual imaging." J Oral Maxillofac Surg **67**(10): 2080-92.

Swennen, G. R., M. Y. Mommaerts, et al. (2009). "A cone-beam CT based technique to augment the 3D virtual skull model with a detailed dental surface." Int J Oral Maxillofac Surg **38**(1): 48-57.

Swennen, G. R., F. Schutyser, et al., Eds. (2005). Three-Dimensional Cephalometry: A Color Atlas and Manual Springer.

Tng, T. T., T. C. Chan, et al. (1994). "Validity of cephalometric landmarks. An experimental study on human skulls." Eur J Orthod **16**(2): 110-20.

Troulis, M. J., P. Everett, et al. (2002). "Development of a three-dimensional treatment planning system based on computed tomographic data." Int J Oral Maxillofac Surg **31**(4): 349-57.

Trpkova, B., P. Major, et al. (1997). "Cephalometric landmarks identification and reproducibility: a meta analysis." Am J Orthod Dentofacial Orthop **112**(2): 165-70.

Tucker, S., L. H. Cevidanes, et al. "Comparison of actual surgical outcomes and 3-dimensional surgical simulations." J Oral Maxillofac Surg **68**(10): 2412-21.

Uechi, J., M. Okayama, et al. (2006). "A novel method for the 3-dimensional simulation of orthognathic surgery by using a multimodal image-fusion technique." Am J Orthod Dentofacial Orthop **130**(6): 786-98.

Xia, J., H. H. Ip, et al. (2000). "Computer-assisted three-dimensional surgical planning and simulation: 3D virtual osteotomy." Int J Oral Maxillofac Surg **29**(1): 11-7.

Xia, J. J., J. Gateno, et al. (2007). "Accuracy of the computer-aided surgical simulation (CASS) system in the treatment of patients with complex craniomaxillofacial deformity: A pilot study." J Oral Maxillofac Surg **65**(2): 248-54.

Xia, J. J., C. V. Phillips, et al. (2006). "Cost-effectiveness analysis for computer-aided surgical simulation in complex cranio-maxillofacial surgery." J Oral Maxillofac Surg **64**(12): 1780-4.

Appendices

A. Orientation Protocol

ORIENTATION PROTOCOL

<u>Orientation 1: Modified Frankfort Horizontal</u>

- Origin: Sella prime
- Horizontal plane: modified 3D Frankfort based on 3 points: both right and left orbitale and right porion
- Midsagittal plane: sella to nasion
- Frontal plane: dropped from Sella prime perpendicular to other two planes

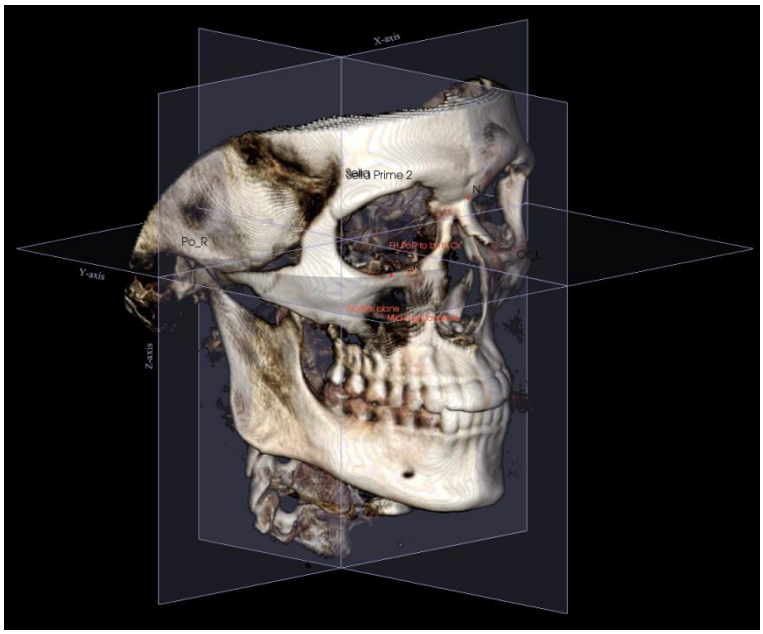

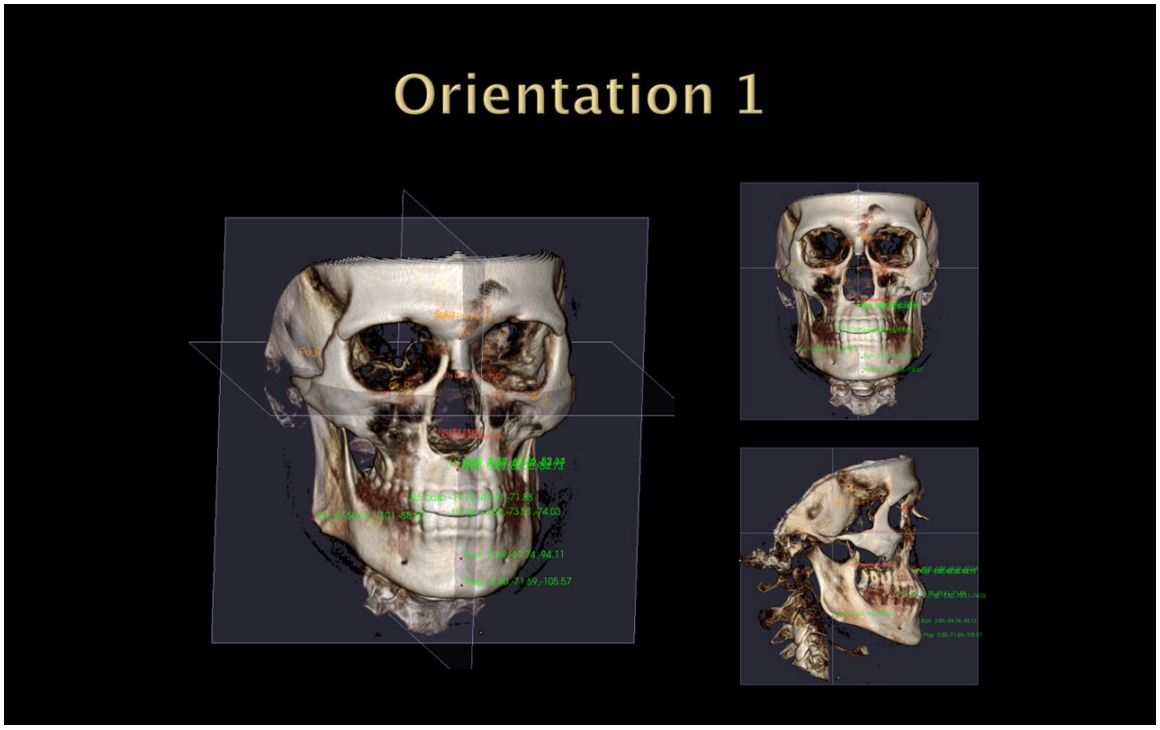

Settings:

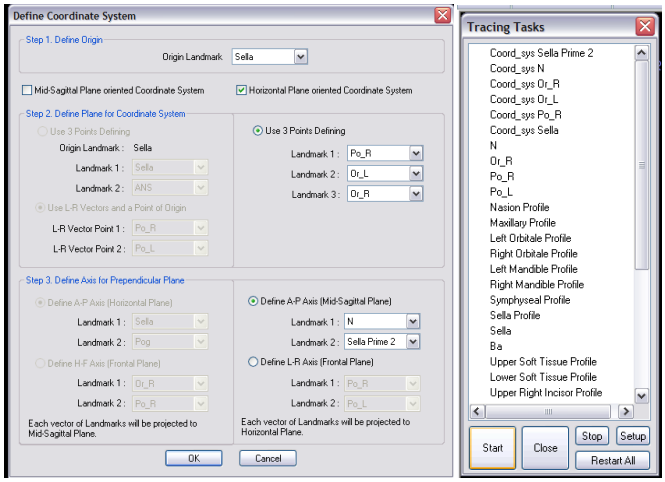

Sella Prime 2:

1. Default view consists of an axial clipping with Grayscale volume rendering

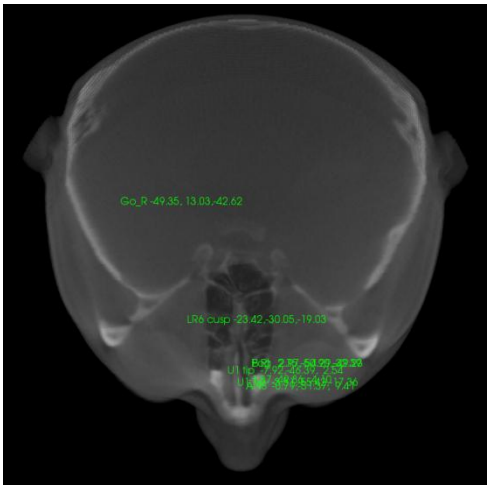

2. Switch to sagittal view to get the approximate height of the axial clipping (although the midsagittal location of the landmark is more important than the height for this landmark as it is used to create the midsagittal plane).

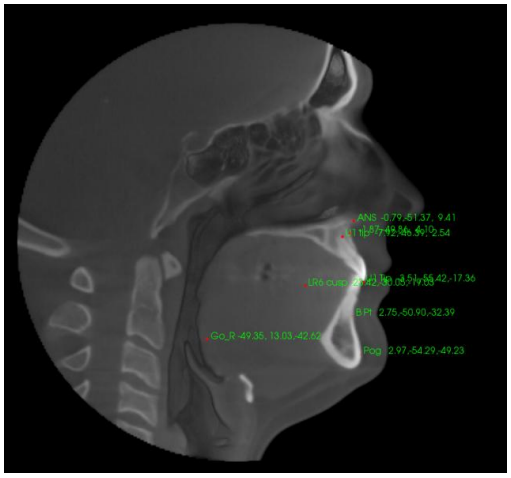

3. Switch to axial to check clipping

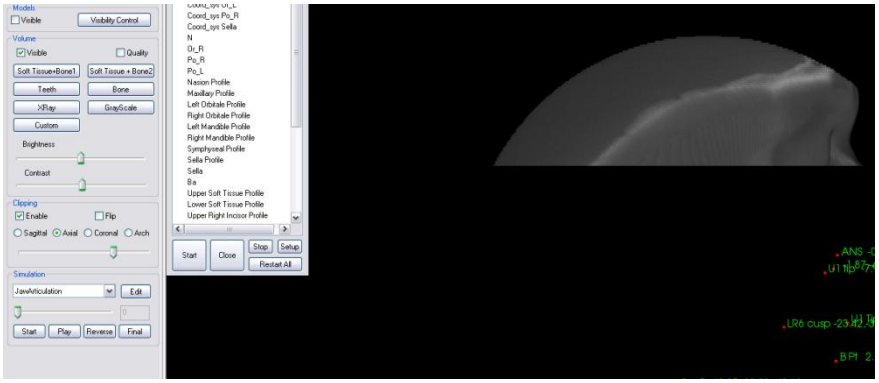

4. Then place Sella Prime 2 in midsagittal center of original view, which should now be at the right height

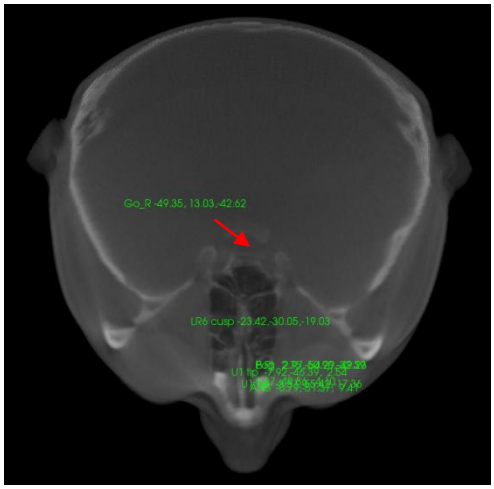

Nasion:

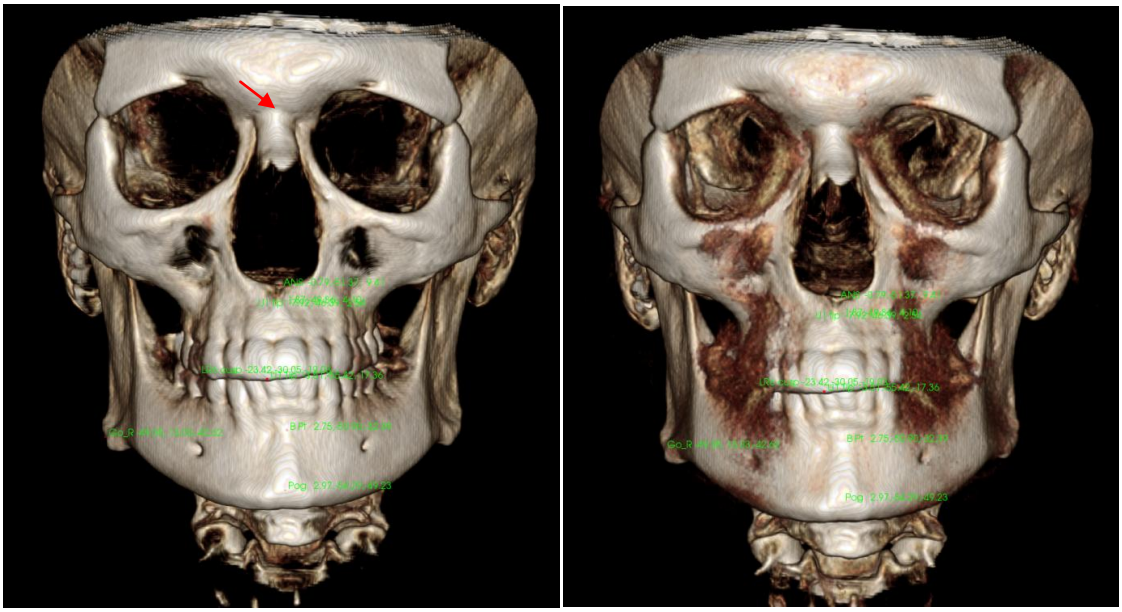

Zoom and tilt as needed to evaluate nasion contour; increase opacity to visualize the bone without too much noise. The second image has too much noise here.

Orbitale:

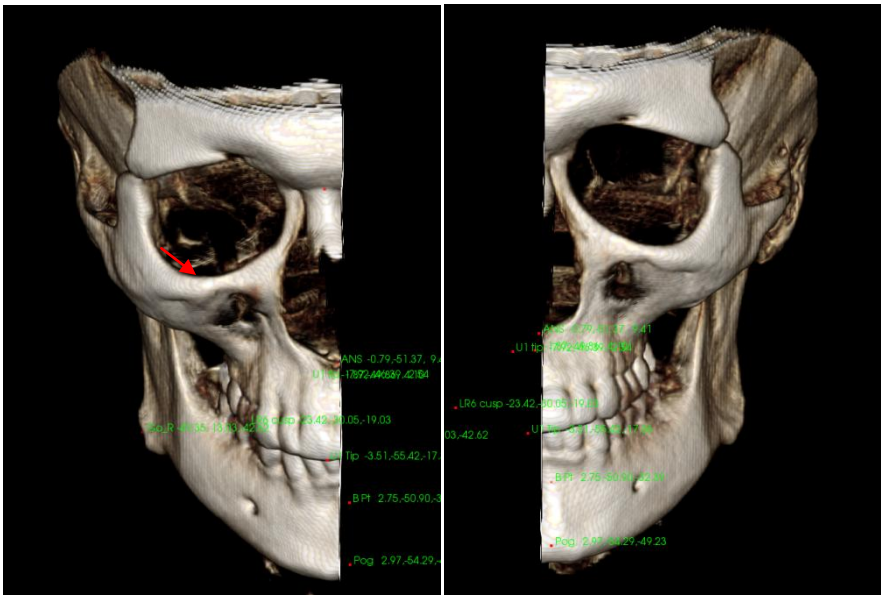

Identify most inferior point on anterior border of the orbit.

Porion:

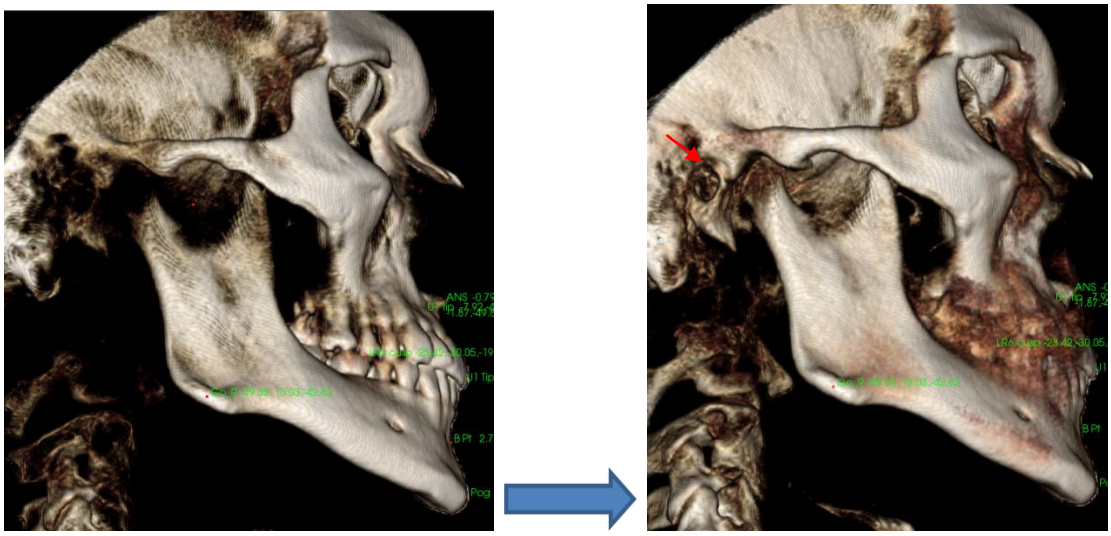

Increase brightness until it is possible to determine the superior border of porion, without too much noise at porion, disregard noise around dentition; tilt as needed

Sella Prime:

Scroll wheel until Sella Prime 2 is just visible to ensure clipping is at midsagittal plane

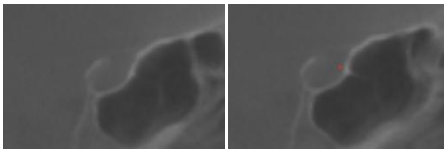

Then pick Sella Prime at the point of greatest convexity on the most superior anterior portion of the hypophyseal fossa

Orientation 2: Anatomage Original Default

- Origin: Nasion
- Midsagittal plane: Perpendicular plane to a line connecting right and left porions through nasion
- Horizontal plane: 3D Frankfort using right porion and right orbitale, and perpendicular to midsagittal plane
- Frontal plane: dropped from nasion perpendicular to other two planes

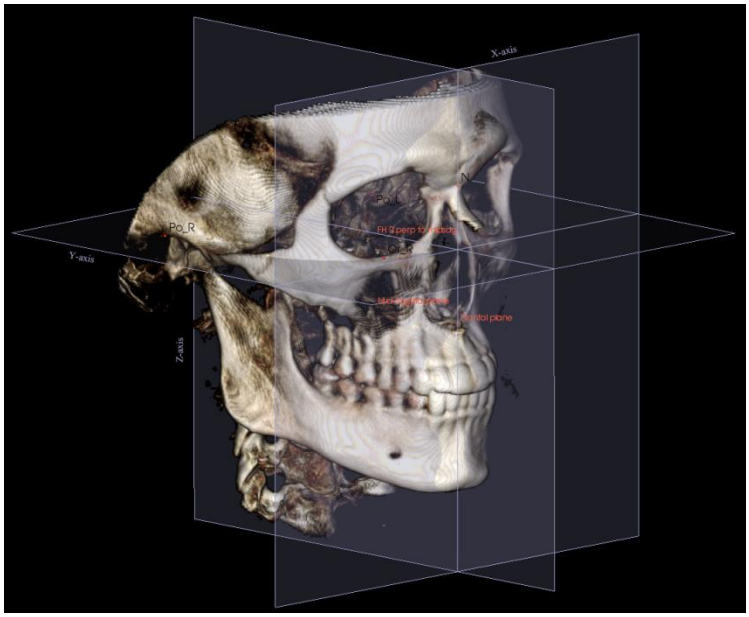

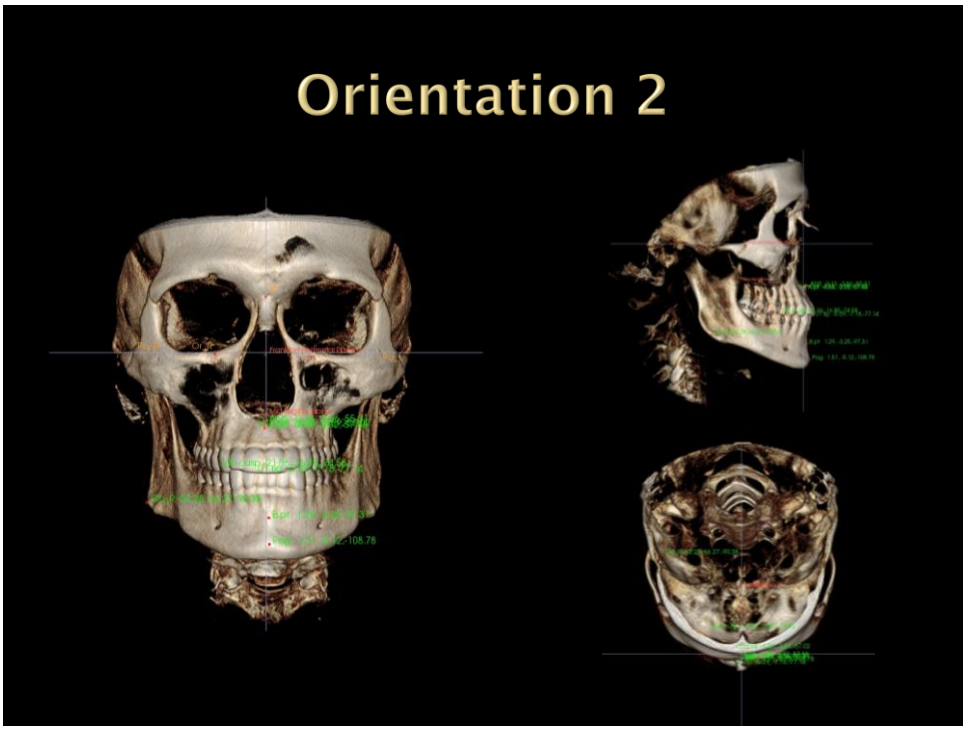

Settings:

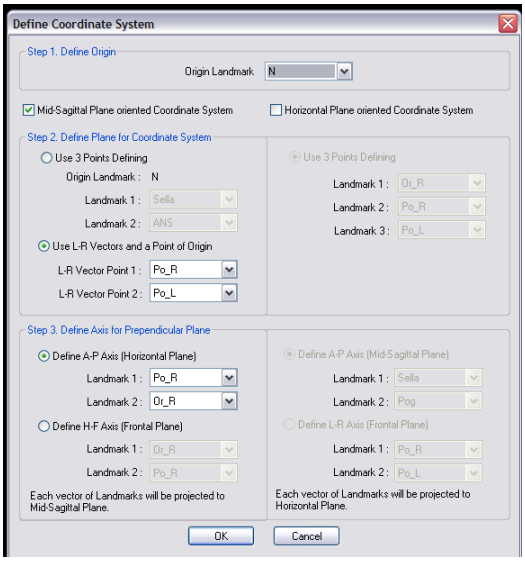

This technique requires only the identification of nasion, right and left porions and right orbitale. Identify these landmarks by following the same instructions for these points in Orientation 1.

Orientation 3 – UCSF Planar View

- Origin: Sella Prime
- Horizontal plane – 2 pts: sella and nasion AND parallel to a line connecting frontozygomatic (Fz) sutures
- Midsagittal plane – 2 pts: opisthion and crista galli AND perpendicular to horizontal plane
- Frontal plane – origin pt (sella prime) AND perpendicular to both horizontal and midsagittal planes
- Created in section views, as opposed to 3D cephalometry tool as other 3 orientation methods

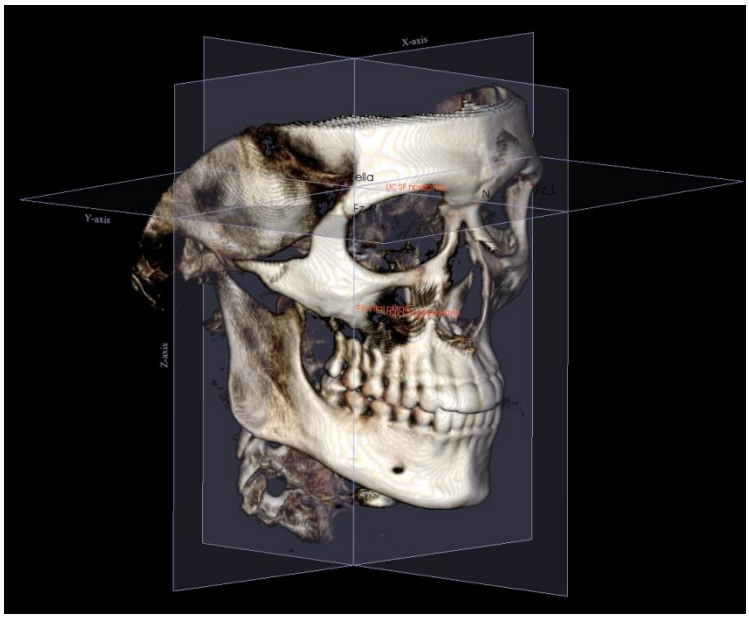

1. Open Section view, click orientation icon.

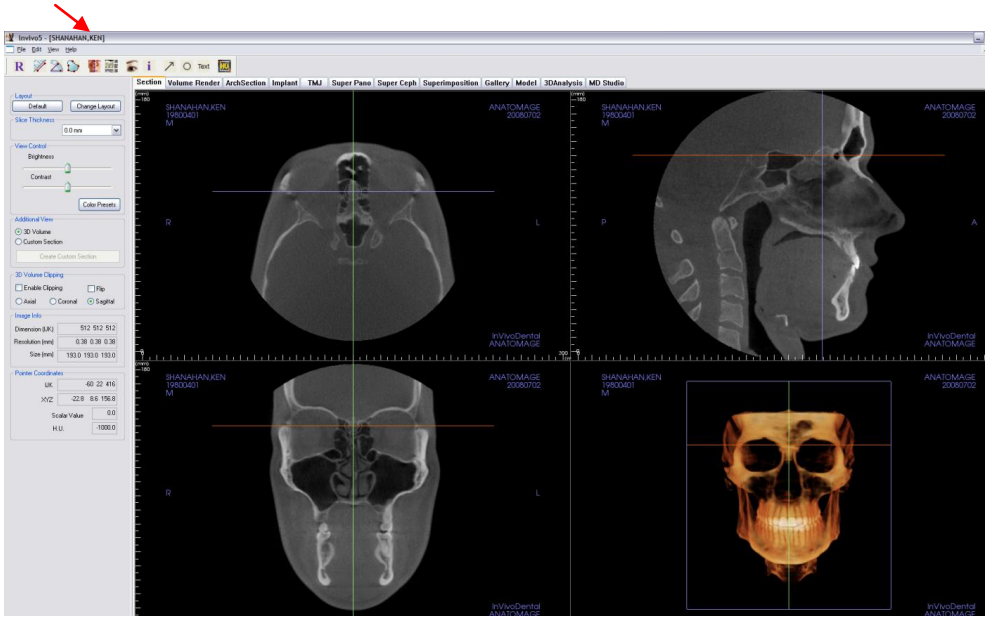

2. Set orientation so that horizontal line in each planar view bisects the 2 landmarks listed below for each of the views. Sequence: sagittal to axial to coronal, and then continue back through sequence as many time as needed until satisfied.

   - Coronal: most medial point of the frontozygomatic sutures bilaterally
   - Axial: opisthion to crista galli
   - Sagittal: sella to nasion

3. Set origin point: Go to Volume view, set Preset to Grayscale, clip sagitally to 50%, view from sagittal, and place 3D landmark at sella prime.

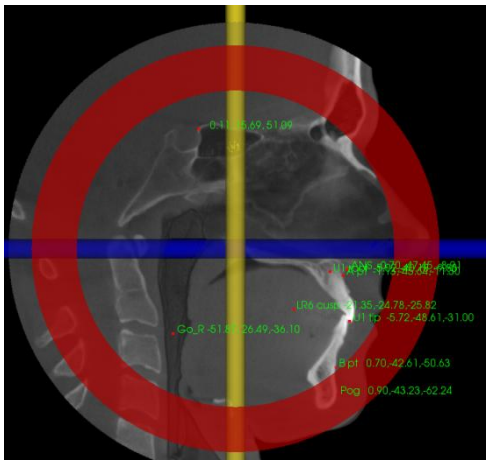

4. Click orientation icon, move orientation axis by holding Ctrl and moving each axes independently until 3D landmark reads (0.00,0.00,0.00).

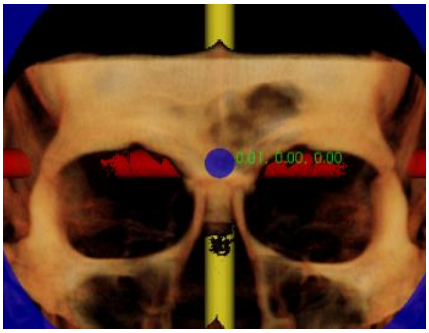

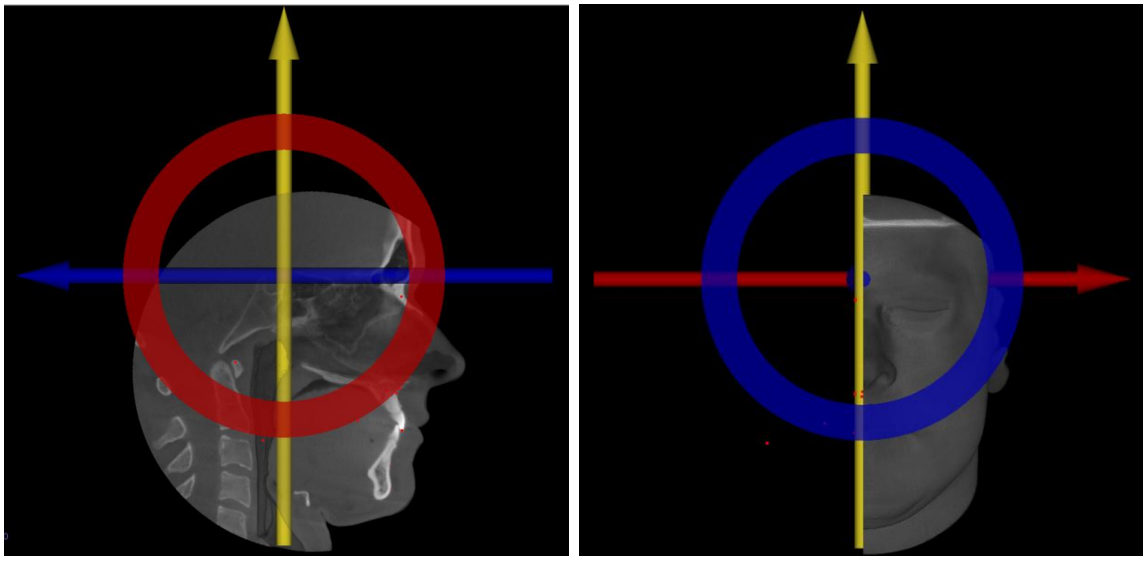

NFZ Based Orientation

- Origin: Nasion
- Horizontal plane: defined by 3 points: nasion and both frontozygomatic sutures
- Midsagittal plane: parallel to crista galli-clivus line passing through nasion and perpendicular to horizontal plane
- Frontal plane: perpendicular to the other 2 planes through nasion

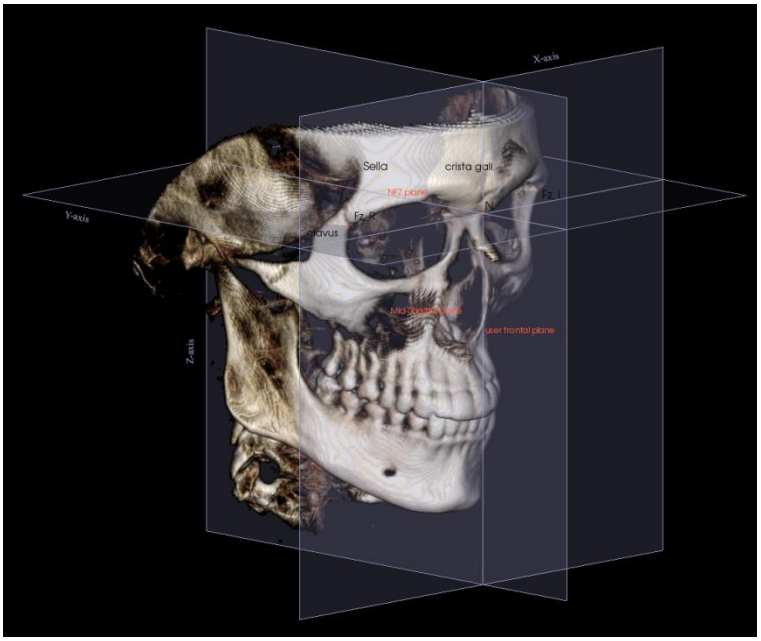

Settings:

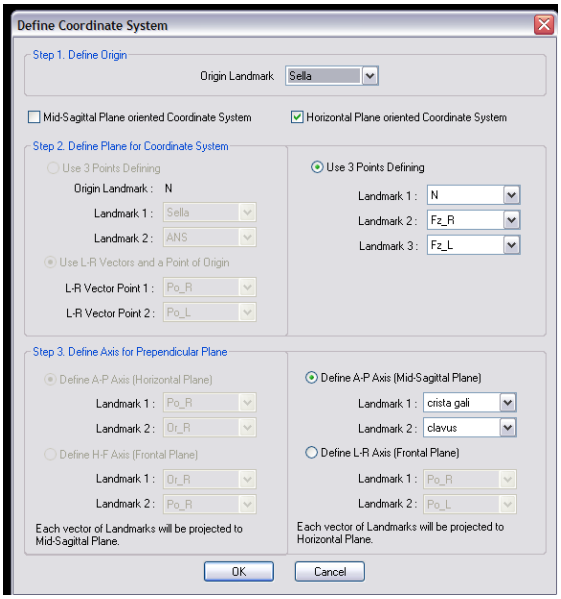

1. Identify nasion as described above
2. Identify the most medial point of the frontozygomatic sutures bilaterally, as shown below.

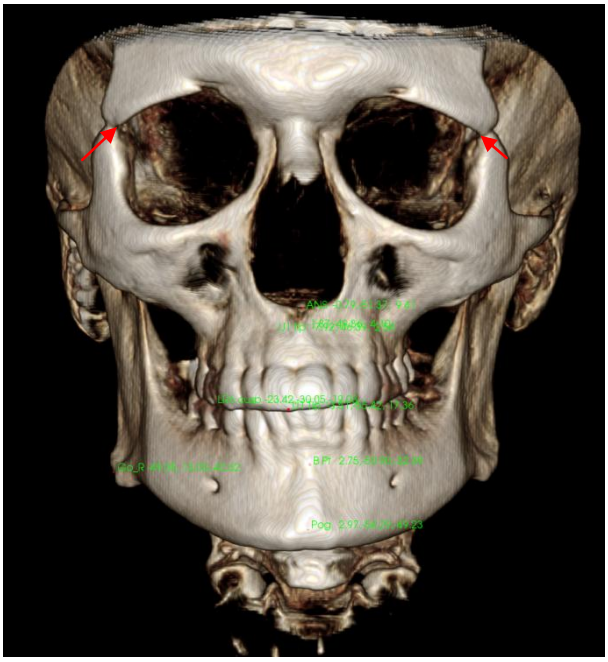

3. Using axial view with axial clipping, identify clivus, the most inferior point in the shallow depression behind the dorsum sellae, which slopes obliquely backward, and is continuous with the groove on the basilar portion of the occipital n the volume.
4. Identify the most superior point of the perpendicular plate of the crista galli on the volume using axial view with axial clipping. Switch between grayscale and bone presets as needed to visualize this point.

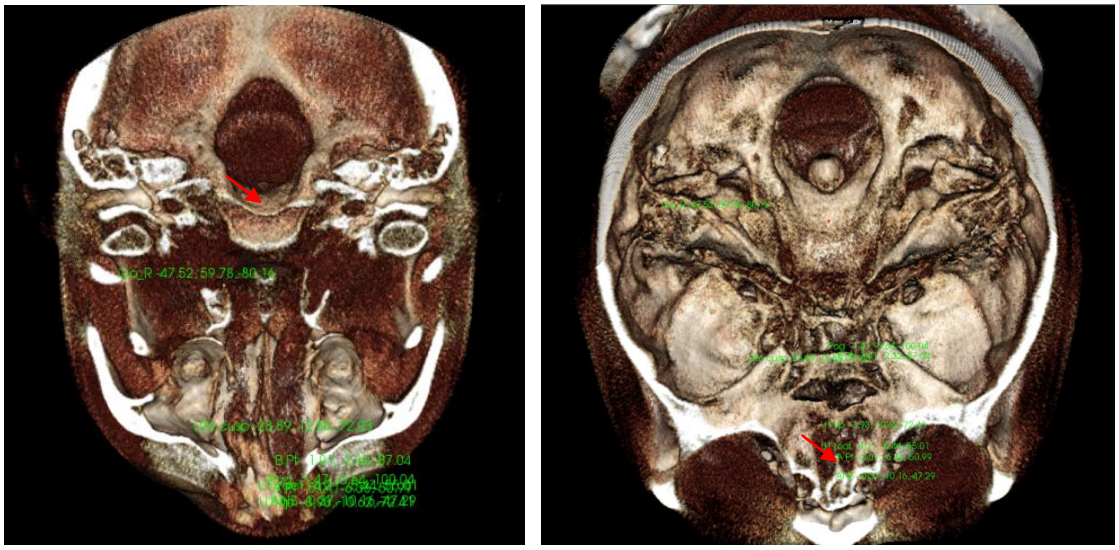

Figure. Left) Identify clivus with axial clipping of bone preset view. Right) Identify crista galli anteriorly using same view with a higher axial clipping.

Publishing Agreement

It is the policy of the University to encourage the distribution of all theses, dissertations, and manuscripts. Copies of all UCSF theses, dissertations, and manuscripts will be routed to the library via the Graduate Division. The library will make all theses, dissertations, and manuscripts accessible to the public and will preserve these to the best of their abilities, in perpetuity.

Please sign the following statement:

I hereby grant permission to the Graduate Division of the University of California, San Francisco to release copies of my thesis, dissertation, or manuscript to the Campus Library to provide access and preservation, in whole or in part, in perpetuity.

Author Signature

6/9/11

Date